Hydrogel Toughening Strategies for Tissue Mimicking Materials

Chukwunonso Moneme

A Thesis

in

The Department

of

Chemical and Materials Engineering

Presented in Partial Fulfillment of the Requirements

for the Degree of Master of Applied Science (Chemical Engineering) at

Concordia University

Montreal, Quebec, Canada

August 2024

CONCORDIA UNIVERSITY

School of Graduate Studies

This is to certify that the thesis prepared

By: Chukwunonso Moneme

Entitled: Hydrogel Toughening Strategies for Tissue Mimicking Materials

and submitted in partial fulfillment of the requirements for the degree of

Master of Applied Science (Chemical Engineering)

complies with the regulations of the University and meets the accepted standards with respect to originality and quality.

Signed by the final Examining Committee:

_____ Chair

Dr. Patricia Comeau

_____ Examiner 1

Dr. Martin Pugh

_____ Supervisor

Dr. Paula Wood-Adams

Approved by _____

Dr. Zhibin Ye

September 4, 2024 _____

Dr. Mourad Debbabi

ABSTRACT

Hydrogel Toughening Strategies for Tissue Mimicking Materials

Chukwunonso Moneme

Hydrogels are a class of material that have garnered a great deal of attention across the domain of tissue engineering as potential candidates for tissue mimicking materials. Their softness and customizability make them very versatile in their applications and allows their specific properties to be optimized based on the intended applications. This thesis explores the viability of hydrogels as tissue mimicking materials. First, a comprehensive literature review introduces the mechanical properties of the soft tissues around the knee, specifically skin, muscles, ligaments, tendons, and cartilage. This chapter also outlines different strategies used to improve the performance of hydrogels in mimicking the soft tissues around the knee, which is the biggest joint in the human body. Next, the experimental section of the thesis outlines the development of a hydrogel using solvent exchange and annealing. This chapter discusses the improved compressive mechanical properties of the developed hydrogel, as well as the impacts of glycerol and thermal annealing on the hydrogel.

Acknowledgements

I would like to acknowledge the help and support of my lab group throughout the development of this thesis. First, thank you to Bianca Martins for assisting me in interpreting some of the FTIR results. Thank you to Abdolali Mehrjou for his contributions to the review paper included in the literature review. Thank you to Milad Hadaeghnia for teaching me so much about hydrogels and material characterization. A huge thank you to Prof. Paula Wood-Adams for all of her guidance and education throughout this project.

Lastly, I would like to thank my family and friends for their consistent support and encouragement along this journey

Dedication

This thesis is dedicated to my two grandfathers, now passed, Prof. Emmanuel Uche Odigboh, and Prof. Paul Chuka Moneme.

Contribution of Authors

Chapter 2:

Abdolali Mehrjou contributed the main content of the Muscles, Tendons, and Ligaments sections of the literature review, and the Tendons and Ligaments and Muscles sections of the Hydrogel Models section. Milad Hadaeghnia provided the general outline for the review paper and provided insights throughout the development of the paper. Prof. Wood-Adams assisted with final reviewing and editing of the review paper. All of the other content in the review paper, including the formatting, referencing, and majority of the editing, was conducted by myself.

Chapter 3:

The conception, research, and execution of the study in Chapter 3 was conducted by me. Prof. Wood-Adams helped with the interpretation of the data as well as the editing of the paper.

Table of Contents

List of Figures

List of Tables

1. Introduction

1.1. Background

Tissue engineering is a growing discipline that concerns the development and assembly of constructs that can be used to repair, replace, or reinforce tissues and organs in the body [1]. This can include biomaterials that are developed for implantation, such as scaffolds and grafts, or materials used *in vitro* to as models and training tools. Regardless of the application, an important challenge facing the discipline and field is the development of synthetic materials that can effectively mimic the mechanical properties of biological tissues.

There have been many different types of materials used to simulate human tissues, including liquid suspensions, foams, elastomers, and resins [2]. Hydrogels, which are networks of polymers that exist within an aqueous membrane, have gained attention as good candidates for tissue mimicking materials due to their versatility and biocompatibility. Hydrogels are already commonly used across the biomedical industry in drug delivery, cellular scaffolding, and beyond [3]. They are especially attractive for mimicking soft tissues, such as skin and muscle, that require mechanical strength as well as flexibility and softness. Conventional hydrogels, however, tend to possess lower moduli than biological tissues and are not particularly resilient under repetitive mechanical loading compared to their biological counterparts. Many techniques and strategies have been developed over the years to toughen hydrogels to make them more viable candidates for tissue replacement in the body. These strategies vary greatly depending on the intended application for the hydrogel, as well as the specific characteristics of biological tissues that the hydrogel is meant to mimic.

The development of hydrogels as tissue mimicking materials has great implications for the medical community and stands to significantly improve the quality of life for many people. A common area where hydrogels could be used to improve people's health is as prostheses and implants. Knee surgeries, for example, are one of the most common surgeries in Canada and are significant, life-changing surgeries [4]. These surgeries are most often caused by osteoarthritis, which is the result of gradual loss of articular cartilage in the knee [5]. As the largest joint in the body, the knee is essential to movement, and osteoarthritis and cartilage degradation can lead to disability and immobility. Currently, knee replacements are most commonly a combination of plastic and metallic components that replace the cartilage and some bone tissues. These prostheses can be stiff and uncomfortable, but with a softer replacement like a hydrogel, that discomfort could be lessened [4]. Moreover, the reduction of inorganic components in the body can reduce the risk of negative reactions and rejection of the prosthesis by the body.

1.2. Objective

The objective of this research was initially to develop a model of the human knee, using polyvinyl alcohol (PVA) hydrogels to simulate all of the soft tissues, namely skin, cartilage, muscles, tendons, and ligaments. After a change in available resources, the scope of research was redefined to explore the efficacy of different toughening strategies on the development of cartilage mimicking hydrogels. Upon reviewing existing toughening strategies, annealing was selected as a suitable technique in the development of hydrogels for compressive loading, due to a lack of data in the literature around the efficacy of annealing in compressive applications. This investigation sought to determine whether similar trends could be observed in compressive environments, as in tensile, and whether annealing would be an effective technique for the development of cartilage mimicking hydrogels. This was accomplished by adopting a technique from Wu et al. that employed a solvent exchange process to improve the effects of annealing on PVA hydrogels.

1.3. Thesis Format

This thesis is structured into 5 main sections. This first section introduces the concepts of hydrogels and provides an overview of the motivation and objectives of the research conducted. Chapter 2 contains a comprehensive review of the relevant literature in the field, presented as a manuscript of a review paper that is to be submitted for publishing. This includes information on the physical structure and functions of the soft tissues in the knee, and an overview of the techniques and strategies used to develop materials to mimic these tissues. Chapter 3 presents the experimental section of this thesis, which has also been formatted as a manuscript to be submitted for publication. This chapter outlines the development of hydrogels with improved compressive mechanical properties and an explanation of the changes that the gel undergoes through the solvent exchange and annealing processes it undergoes. Chapter 4 includes some conclusions to tie together the main takeaways from Chapters 2 and 3 and discusses potential future research and further development of the research included in this work. Lastly the final section presents a bibliography of the sources used throughout this thesis that informed the research and experimentation conducted.

2. Literature Review

This chapter explores a number of systems used in the development of tissue mimicking materials. This includes an identification of the structure, function, and mechanical properties of soft tissues in the knee, and explores strategies that researchers use to achieve similar properties in hydrogels. The benefits and drawbacks of hydrogels in tissue engineering are also presented and discussed.

A review of hydrogel-based systems for tissue mimicking materials

Chukwunonso Moneme, Abdolali Mehrjou, Milad Hadaeghnia, Paula Wood-Adams

Abstract

Hydrogels are attractive candidates in the field of biomedical and tissue engineering for replicating tissues in the body. The 3D nature of the gels, as well as their tunability, biocompatibility, and flexibility make hydrogels suitable to mimic soft tissues like skin and muscles. From a mechanical perspective, however, hydrogels in their most basic state do not possess the mechanical properties required to effectively simulate tissues in the body. As such, researchers have developed strategies to toughen hydrogels and improve their mechanical properties, making them more analogous with natural tissues. In this review, the structure, function, and mechanical properties of soft tissues in the knee are identified, and the strategies that researchers use to achieve similar properties in hydrogels are discussed. The benefits and drawbacks of hydrogels in tissue engineering are also mentioned, exploring areas for further development in the field.

Key words: hydrogel; tissue mimicking; mechanical properties; biomimicry

Introduction

Within the realm of tissue engineering, the development of materials that effectively mimic organs and tissues within the human body is a critical area of interest. These biomimicking materials can be used as surgical models and training materials or even scaffolds and implants in the body. When used outside of the human body as models, these materials can help develop tools and train surgeons in an environment that is more representative of human anatomy. Within the human body, these replicas can be used as prostheses to improve the quality of life of people who have experienced loss or deterioration of certain parts of their body.

There are many different types of materials that have been used to mimic tissues in the body, such as foam, rubber, and plastics. Hydrogels, which are networks of polymers that exist within an aqueous membrane, have been garnering increased interest as candidates for tissue mimicking materials due to their versatility and biocompatibility. Hydrogels have already been used in biomedical applications as drug delivery agents, cellular scaffolds, and beyond. Hydrogels are particularly interesting in their ability to replicate the biomechanical properties of soft tissues such as skin and muscles. Their tunability and customizability make them attractive candidates for developing grafts and implants that can move with the body. Generally, however, hydrogels do not possess the mechanical strength and resilience necessary to fully replace the complex soft structures in the body.

To functionalize hydrogels as replicas for soft tissues, different strategies can be used to modify and strengthen the bare hydrogel matrix. Due to the versatile nature of hydrogels and the broad spectrum of polymers that can be used to develop them, there are many different approaches that can be combined and customized to achieve the specific qualities required for a unique application. While there are commonalities amongst the compositions of biological tissues, they are all quite complex and contain different features that contribute to their mechanical properties.

This review paper explores strategies used to toughen hydrogels and improve their mechanical properties, specifically for the purpose of simulating biological tissues. The techniques reviewed in this paper may have applications across the domain of tissue engineering, from *in vitro* models to *in vivo* grafts. For the purpose of this paper, the tissues included are those in the knee, which is the body's largest joint and one of its most complex. This includes skin, muscle, tendons, ligaments, and cartilage, but does not include hard tissue such as bone.

Structure and Mechanical Properties

Skin

Skin is the largest and most superficial organ in the human body. It acts as a barrier to external conditions, protecting the body from injury and radiation, and regulates the exchange of energy and moisture across the skin's barrier. The organ itself is composed of three distinct layers, each with its own components and function.

The first and deepest layer is the hypodermis, or subcutaneous layer, which connects the more superficial layers of the skin to interior structures such as muscles and bones. The hypodermis contains a significant amount of fat cells that are organized into adipose lobules, which store energy, as well as other components such as hair follicles and blood vessels [6]. Superficial to the hypodermis is the dermis, which is a fibrous layer of connective tissue that provides strength and flexibility to the skin. The dermis is composed of the papillary dermis and the reticular layer, from least to most deep respectively [7]. Collagen is the main component of the dermis and is principally responsible for providing tensile strength and pliability to the skin. Elastic fibers, as their name suggests, provide the skin with elasticity [8]. The third and most superficial layer of the skin is the epidermis. This layer plays an important role in protecting the body. The epidermis comprises five strata: basale, spinosum, granulosum, lucidum, and corneum. With these strata combined, this layer acts as a semipermeable barrier against the external environment, defending against foreign physical and chemical agents, while permitting the exchange of moisture, energy, and nutrients across the skin's barrier [9].

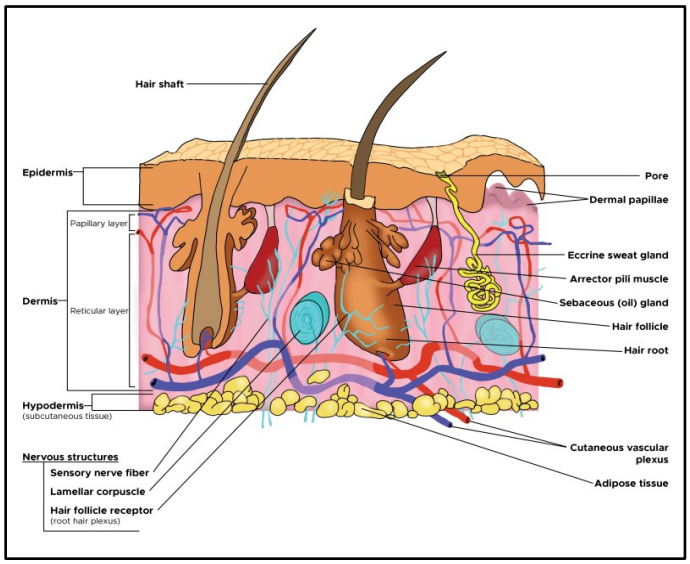

Figure 2.1: Layered diagram of skin and its internal structures [9].

While human skin may seem like a relatively simple organ, its layered design provides it with many important biochemical and biomechanical properties such as elasticity and water barrier properties. For the scope of this review, some of the key biomechanical properties of skin are its tensile and compressive moduli, as well as its tear strength. These values can vary greatly depending on the source of skin analyzed and its combination of parameters including, but not limited to, age, race, and sex of the individual as well as the location on the body that the skin originates from. Kalra A. et al. report a number of different literature values for the tensile modulus of skin, ranging from 4.02 MPa in the abdomen to 140 MPa in the forehead [10]. This report also summarized values for skin's compressive modulus ranging from 4.75 - 89.4 kPa. In an investigation into the tear resistance of skin, Yang et. al. report values ranging from 8 - 28 MPa [11]. These properties mainly come from the dermis and epidermis where collagen provides the skin with pliability and resistance against compressive and tensile forces, and elastin provides elasticity to the skin. The more superficial layers of the epidermis also contain spiny cells and horny scales that provide tear and puncture resistance to the skin [8].

A key mechanical property of skin is its self-stiffening ability. This property is anisotropic in nature and dependent on the direction of force applied relative to the Langer's lines, which indicate the directions where the skin is under the most tension [11]. Ni Annaidh et al. reported an ultimate tensile stress of 17 – 28 MPa parallel to the Langer lines, and 10 – 16 MPa perpendicular to them [12]. Figure 2.2 demonstrates the structure of collagen in the skin under different levels of tensile strain. In the toe region (Phase I) the collagen is relaxed, and its fibers are wavy. Here, the skin acts almost isotropically and there is a linear relationship between stress and strain. This phase also sees a relatively low elastic modulus between 0.1-2 MPa. As the force applied is increased (Phase II), the collagen fibers unfurl and elongate in the direction of the load. This is more representative of the natural state of the skin's collagen since skin is normally under some tension in vivo. As the tensile forces continue to increase (Phase III), the collagen becomes fully elongated, and the stress-strain relationship becomes linear again as the collagen strongly resists the tensile forces [10]. Beyond this point, the fibers in the skin begin to break and skin starts to rip [13]

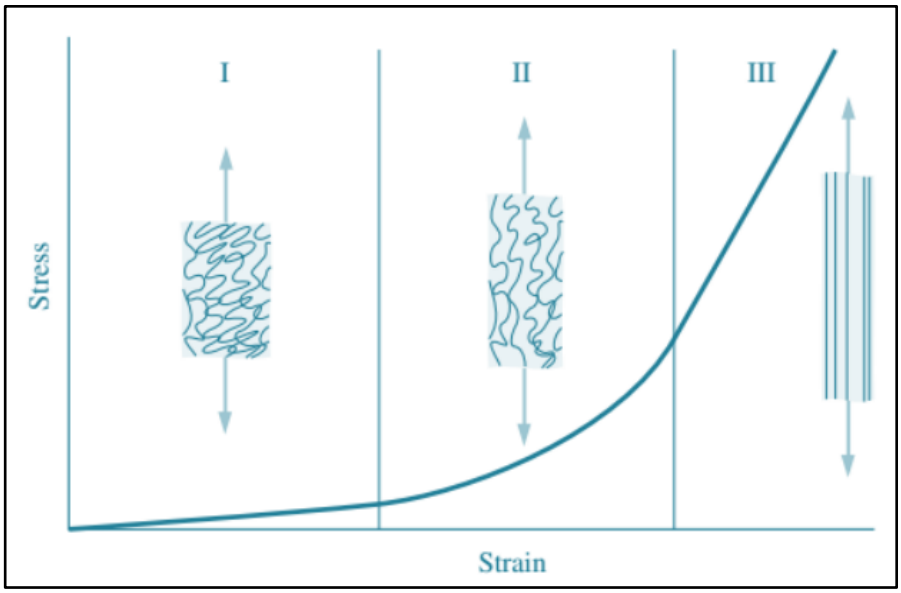

Figure 2.2: A representation of the structure of collagen in the skin throughout tensile testing [10].

Cartilage

Cartilage is an avascular and aneural tissue that exists on the head of bones. Its main purpose is to protect the bone by opposing compressive forces, providing support to the bone, and improving bone resilience. Structurally, cartilage is a matrix composed of fibrous tissues, water, collagen, and proteoglycans, as well as other proteins [14]. This matrix enables cartilage to retain water and maintain its characteristic mechanical properties [15].

Four different zones can be identified within cartilage due to a gradient in the concentration of chondrocytes. Each zone, namely the superficial, middle, deep, and calcified zones, contain a pericellular, territorial, and interterritorial region. The different regions mainly serve different biological functions including signal transduction, but the different zones contribute significantly to the mechanical properties of articular cartilage. The superficial zone protects the deeper cartilage by resisting shear, tensile, and compressive forces. This is possible because the collagen fibers of this zone are densely packed parallel to the surface, putting it in direct contact with synovial fluid. This zone constitutes 10 - 20% of the articular cartilage. The second most superficial zone is the middle or transitional zone. This zone contains thicker collagen fibers and a lower density of chondrocytes. The collagen in this zone is organized in an oblique fashion and it mainly serves to resist compressive forces. The transitional zone constitutes between 40 and 60% of the articular cartilage. Deep to the transitional zone is the deep zone, which sees collagen fibrils organized perpendicular to the articular surface, which provides significant resistance to compressive forces. This zone has the thickest collagen fibers, highest protein content, the lowest water concentration,

and the chondrocytes are organized in columns perpendicular to the cartilage surface. This zone makes up around 30% of the articular cartilage. Lastly, the calcified zone is largely void of chondrocytes, and it mainly serves to secure the rest of the cartilage to the surface of the bone [15].

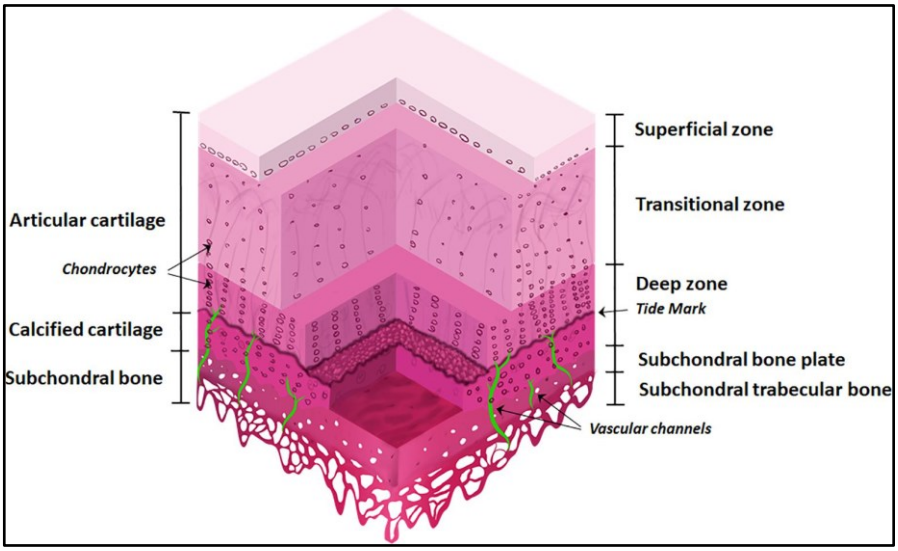

Figure 2.3: Layered Diagram of Articular Cartilage [16].

Muscles

In the body, muscle provides strength and support to the body, while protecting deeper structures like bones and organs. Approximately 40% of the mass of the human body is composed of skeletal muscle [17]. It is known that it produces mechanical force, which may be applied, for example, for movement and posture, allowing the individual to participate in various leisure activities as well as occupations. Skeletal muscles also play a crucial role in regulating basal metabolism by storing amino acids and carbohydrates and maintaining body temperature.

Multinucleated tubular muscle fibers (with a size of 100 μm) are the most basic functional units of skeletal muscle [18]. The contractile units of muscle fibers are known as myofibrils. When the myofibril is supplied with energy, the actin filaments and myosin bundles begin to contract. Calcium ions are released from the sarcoplasmic reticulum following stimulation, which binds to troponin C and temporarily displaces tropomyosin. By doing so, the actin-binding sites on myosin are exposed, thereby allowing actin to bind to myosin, which in turn causes the filament to contract and, at a macro level, the muscle itself to contract [17], [18].

Sarcolemma surrounds each skeletal muscle cell or fiber, which is composed of longitudinally oriented myofibrils primarily made up of myosin and actin. A motor neuron's axon contacts the sarcolemma at the neuromuscular junction, where electrical impulses initiate muscle contractions. The endomysium is a layer of connective tissue rich in collagen that separates the different muscle fibers. Generally, collagen fibers are arranged longitudinally in muscle fibers, and the linear orientation is predominant. The perimysium is an outer layer of connective tissue that surrounds different muscle fibers in a fascicle. Likewise, it is composed of a variety of collagen fibers oriented parallel to the muscle fibers beneath, varying in thickness based on the type of muscle. The perimysium is also home to many blood vessels and nerve fibers. The epimysium is the outer layer of connective tissue encircling the entire muscle and contains collagen fibers of a coarser texture than those mentioned earlier [19], [20].

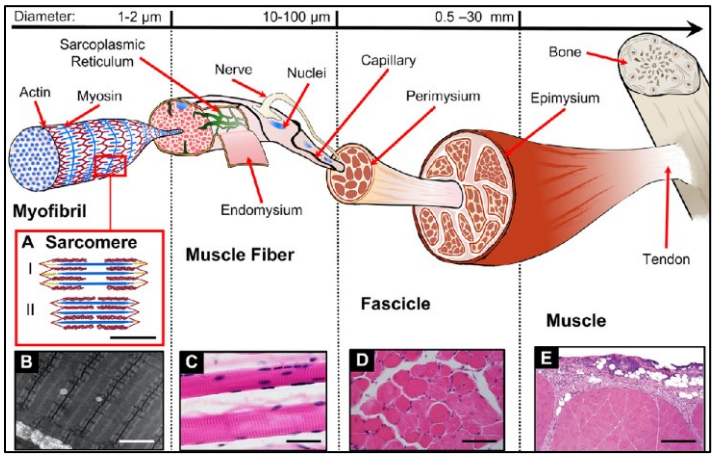

Figure 2.4: Structural diagram of a muscle [21].

Mechanical Properties

The mechanical properties of muscles can be divided into passive and active ones. Passive properties depend only on the response of the tissue during stretching, while active properties arise when the contractile elements are activated during contraction [21]. Skeletal muscle mechanical properties are derived from the tissue mechanical response while stretched and are not always anatomically distinct. The passive mechanical properties are often obtained by imposing an artificial stretch to the muscle, avoiding the activation of the contractile elements. There is a strong connection between muscles' passive properties and the intramuscular connective tissues (epimysium, perimysium, endomysium) and the elastic filaments and titin, which is the most abundant component [17], [22]. *In vitro* stretching of an isolated muscle at different strains results in a passive stress-strain curve. As a result of the mechanical properties of the intracellular and extracellular proteins, like collagen, the muscle exhibits a time-dependent viscoelastic behavior. Skeletal muscles are characterized by their active mechanical properties as a result of their

contractile behavior. The most important attribute of a muscle is the force that it can generate. The muscle develops its maximum force when the sarcomere length is about 2.2 μm (optimal length in humans), and the force decreases as the sarcomere reaches about 175% of its optimal length. The total stress-length relationship is the result of the combination of the passive and active mechanical properties of the muscle [21], [23], [24].

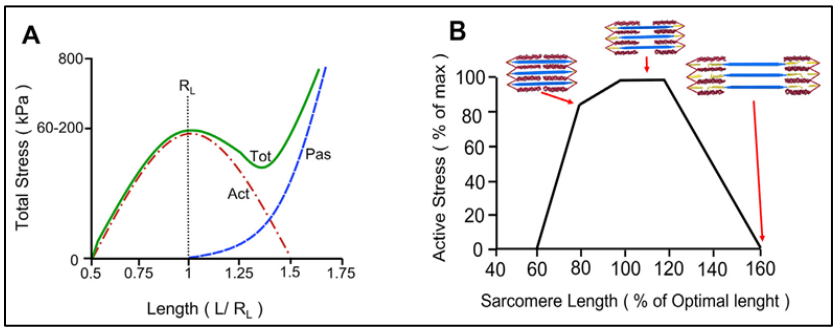

Figure 2.5: Passive and active mechanical behaviors of skeletal muscles A) Total stress-length behavior during a contraction. Length is normalized by the resting length (RL) of the muscle. The total curve (Tot) is the composition of the active curve (Act) and the passive one (Pas). The active curve finds its maximum in correspondence with the optimal length of the sarcomere (RL) [25]. *B) Typical sarcomere active stress (expressed as a percentage of the maximum) compared to the sarcomere length (expressed as a percentage of its optimal length). The active stress is maximum in correspondence of the sarcomere optimal length Lo. The pictures show the different levels of sarcomere overlap* [26].

Tendons

As the main connection between muscles and bones, tendons play a major role in the transfer of forces between muscles and skeletal structures throughout the body. Specifically, there are two main functions of tendon tissue: the first is to transmit force from muscle to bone, and the second is to facilitate movement of the body [27]. Certain tendons, such as the equine superficial digital flexor tendon or the human Achilles tendon, are more functionally complex and therefore allow for more efficient energy storage [28], [29], [30].

In order to determine the characteristics of tendons, it is necessary to examine their multiunit hierarchical structure made up of collagen molecules, fibrils, and various levels of bundles of fiber [31]. Tendons contain tendon fibroblasts, called tenocytes, and stem, or progenitor, cells [32], [33]. Collagen fibers are assembled into subunits of increasing diameter in the structure of a tendon. Triple helices are formed by three collagen molecules, microfibrils are formed by five tropocollagen molecules, and fibrils are bundled into fiber bundles and joined together as fascicles [34], [35]. To ensure minimal friction and preserve the position of the tendon, these subunits are

grouped into fibers, which are then joined together into fascicles [34]. Also, the tendon could glide smoothly to the surrounding structures since the fascicles are surrounded by an epitenon [36].

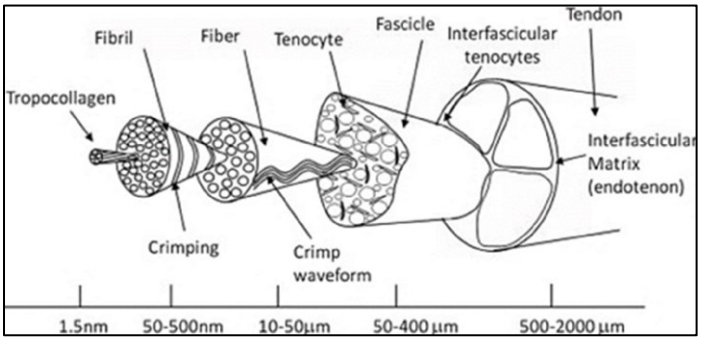

Figure 2.6: Hierarchical structure of tendon [35]. *The collagen fibers of the tendon are organized into subunits of increasing diameter, which creates the hierarchical structure of the tendon. At first, three collagen molecules form a triple helix (also known as tropocollagen). Then, a microfibril is formed by five tropocollagen units, which are linked to make up a fibril. As with many other structures, these fibrils differ in size depending on the role they play in the tendon (varying from 10 to 150 nm)* [34]. *Each fiber is organized into fiber bundles and these bundles are then grouped into fascicles. A crimp is a pattern of undulation created by bundles of fibrils and fibers during embryonic development and functions as a shock-absorbing unit. Finally, a tendon is fabricated when several fascicles are bundled together to form the tertiary bundles, which are enclosed by the epitenon (the fibrous sheath that houses blood vessels, nerves and lymphatics)* [36].

There is a heterogeneous matrix of collagen, proteoglycans, elastin, fibronectin, and fluid encircling tendons. It is important to note that tendon fibers are oriented in parallel to one another, primarily collagen type I, embedded in an extracellular matrix (ECM). This ECM is composed of proteoglycans, glycoproteins, and elastin [37]. A tendon is primarily composed of type I collagen, which is made by specialized fibroblasts. Layered compositions and parallel orientations enable at most tensile strength. Also, Type III collagen is the primary component of the endotenon [36].

Tenocytes are responsible for producing the ECM, assisting with the orientation of newly synthesized fibrils, and controlling the degradation and remodeling of the ECM structure [38]. An important factor in the healing process of tendons is the blood supply [39]. In every tendon of the human body, the toe region of the stress–strain plot is fairly short (2–5%), due to its load transfer function (Figure 2.7).

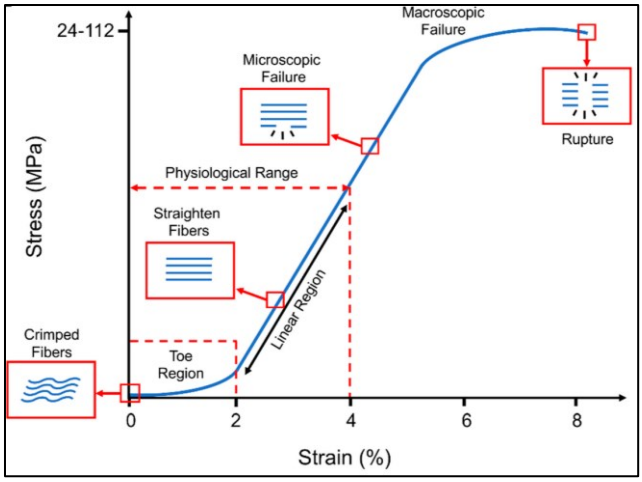

Figure 2.7: Typical stress–strain curve and schematization of the behavior of the collagen fibers for ligaments [40].

It is reported that the patellar tendon can be subjected to 24–69 MPa stress until its failure, while a gracilis tendon can experience stresses up to 112 MPa. Additionally, collagen's weak bonds and the presence of water also contribute to tendons' viscoelasticity [41], [42].

The Achilles tendon can experience forces nearly 70% of its maximum load and stress before it ruptures, despite operating in the toe region of the tissue's stress-strain curve [43]. A correlation has been found between pathology and strength/endurance training in humans, as well as the potential use of functional biomaterial-based tissue replacements in tissue homeostasis [44], [45]. Either low or high mechanical loading of tendons can disturb homeostasis. Stress deprivation reduces cell numbers, decreases tensile modulus, produces inflammatory cytokines, causes matrix degradation, and releases proinflammatory cytokines and vasodilators, resulting in flattening and elongating fibroblasts [46].

Ligaments

Ligaments are responsible for connecting bones, which provide locomotion, and the interface at which they attach to bones is called the enthesis [47], [48]. In addition to providing a means of conveying mechanical stress between mechanically different tissues and maintaining heterotypic cellular communication for interface function and homeostasis, the enthesis contributes to tissue organization and mechanical properties [49], [50]. There are several physiological differences between tendons and ligaments, as well as differences in morphology (which are influenced by the anatomical site) but their composition and hierarchical structure are the same [51].

In addition to being filamentous collagen structures, tendons and ligaments are composed of 80% extracellular matrix (ECM) and 20% cells [52]. The amount of type I collagen in the body ranges

between 60 and 85% [42]. Among the types of collagen present in the tissue, type I collagen provides stiffness and strength, while type III, V, X, XI, XII, and XIV collagens are present in minor quantities and for other purposes [52]. Additionally, Type V collagen and Type III collagen regulate collagen fibril diameter, whereas Type XII collagen has a functional role in tendon repair. Moreover, Type XII collagen bonds with other matrix components, decorin, and fibromodulin [42].

Regarding morphology, as mentioned earlier, tendons and ligaments have similar hierarchical structures. In other words, it is believed that collagen fibrils make up both tendons and ligaments. These fibers coordinate axially with the tendon/ligament and are arranged into different levels of assembly [53]. The collagen fibril is the smallest structural unit of the tendon/ligament tissue, which is produced by tropocollagen molecules aggregation. Fibrils of collagen form collagen fibers, forming primary, secondary, and tertiary fiber bundles, as well as the tendon, which is surrounded by the epitenon and epiligament [54].

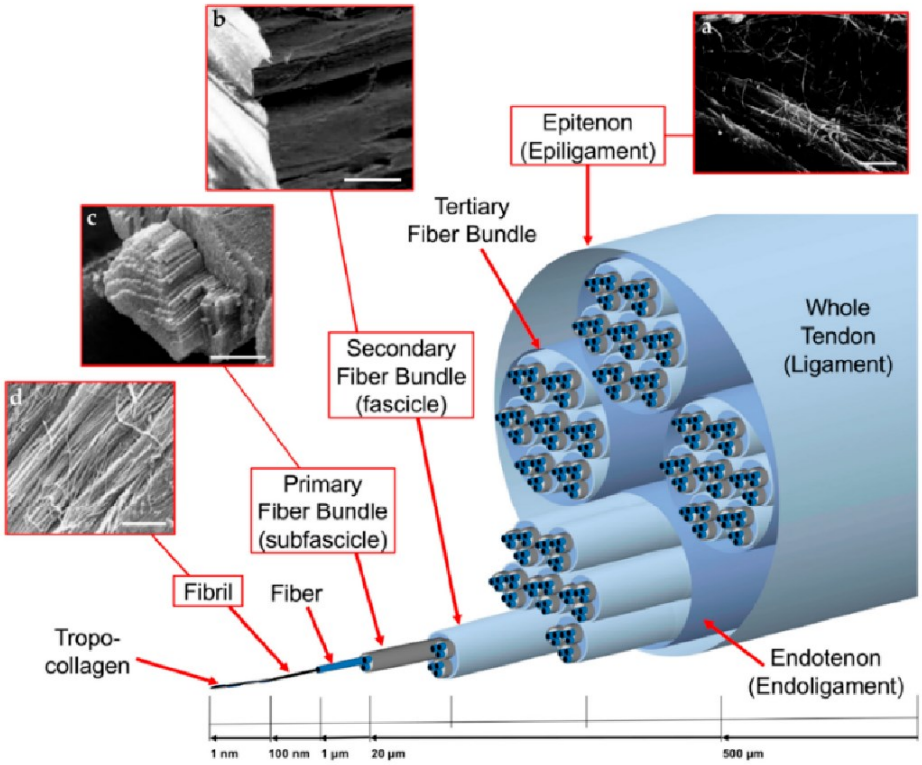

Figure 2.8: Hierarchical structure of ligament [54] *and SEM micrographs from* [53].

Mechanical Properties

Tendons and ligaments possess a hierarchical structure characterized by non-linear mechanical properties. After 2% of strain (toe region), collagen fibers lose their crimped behavior and start

sliding toward one another. The mechanical properties of tendons and ligaments are significantly influenced by the cross-section of the tendon or ligament, the function of the tendon, and the strain rate at which the load is applied. In spite of tendons, ligaments allow different ranges of motions in different joints, and accordingly, the toe region experiences greater strains as a result of specific joints (Fig. 9). For instance, anterior cruciate ligament and spine ligaments undergo 4% and 10–40% of strain, respectively.

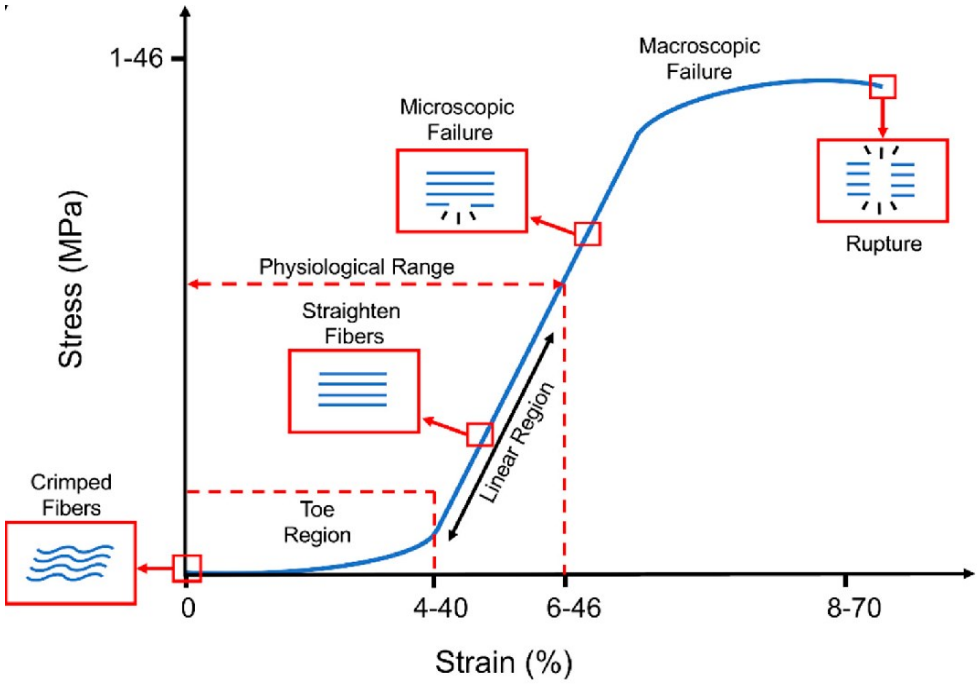

Figure 2.9: Typical stress–strain curve and schematization of the behavior of the collagen fibers for ligaments. Typical ranges of stress and strain are indicated on the x and y axes [40].

The collagen fibers are straightened in the linear region of the stress-strain plots, which provides an ideal elastic recovery when the load is removed. Upon completing the linear region, the fibers gradually begin to slide against each other. As a result of this region, tissue fibers are gradually destroyed until the ligament completely failed. Ligaments can fail under stresses ranging from 1-15 MPa in flavums to 24–46 MPa in lateral collaterals.

Hydrogel Models

A hydrogel, in essence, is a three-dimensional network structure consisting primarily of macromolecules dissolved in water. Depending on the structure and composition of the polymers used, and specifically the presence or absence of covalent interaction and chemical crosslinking points, the hydrogel network can be formed through covalent or non-covalent bonds. Hydrogels are especially attractive in the field of tissue-mimicking materials (TMMs) because of their ease of processing and high degree of tunability. By combining different polymers with various additives, fillers, and crosslinking methods and densities, hydrogels can be altered to mimic a number of biological tissues in the human body.

With respect to preparing hydrogels to mimic biological tissues, there are a number of factors to consider which would affect the performance of the hydrogel produced. First, the type of network formed by polymer(s) can be classified into conventional and unconventional polymer networks. Conventional networks refer to polymer chains connected by permanent covalent bonds, with minimal presence of entanglements, physical crosslinks, and reversible chain connections. Some limitations of conventional network hydrogels include relatively poor mechanical strength and brittle behaviour with low fractur energy compared to other hydrogels. A number of strategies exist that enhance conventional network hydrogels to improve their mechanical properties, resilience, or otherwise make the hydrogels more functional in a desired application. These strategies are quite varied and have produced different subgroupings of hydrogels that each carry their own specific advantages and disadvantages. For the purposes of this review, the strategies explored will mainly be relevant to the optimization of hydrogels for tissue engineering applications. Table 1 below compares the mechanical properties of biological tissues to those reported in the studies of model systems reviewed.

Table 2.1.: Comparison of mechanical properties between biological tissues and hydrogel models.

Tissue	Type	Ultimate Tensile Strength (MPa)	Ultimate Tensile Strain (%)	Young's Modulus (MPa)	References
Skin	Bio	1 - 30	117 – 307	0.5 – 18.8	[10], [11], [12], [13]
	Synthetic	0.347	1731	0.0229	[55]
		0.05	70	8000	[56]
		0.8	914.3	0.2401	[57]
		48.3	100	0.0067	[58]
		0.61	1127	0.063	[59]
Muscle	Bio	0.04 - 0.8	30 - 60	0.03 - 8	[18], [21]
	Synthetic	45	4.2	6784.8	[60]
		2.38	802	0.8	[61]
		1.2	530	2.6	[62]
		0.4 - 3	160 - 310	0.06 – 0.25	[63]
		2.76	2921	0.221	[64]
Cartilage	Bio	10	100	0.5 – 1	[14], [15]
	Synthetic	2.6	34	3.3	[65]
		5.21	572	4.06	[66]
		2.2	270	0.6	[67]
Tendons & Ligaments	Bio	13 - 300	6 - 50	4000 - 8000	[21]
	Synthetic	1.3	<10	7.2	[68]
		0.8	>1000	3	[69]
		7.2	~130	5.4	[70]
		11.10	1879	~10	[71]

Tendons and Ligaments

Due to their structural and functional similarities, many of the approaches used to fabricate hydrogels that mimic tendons and ligaments are quite similar. The main role of tendons is to connect bone to muscle, while ligaments connect bones to other bones. Consequently, both tendons and ligaments consistently experience tensile stress in the human body. Both tissues are anisotropic in nature, meaning that the mechanical behaviour exhibited by the tissues under stress is dependent on the direction of the force applied. When developing hydrogels to mimic these tissues, modifications are often made to simulate the anisotropic nature of the tissues. Achieving anisotropic properties in hydrogels generally involves orienting the polymer chains in the hydrogel to achieve a more ordered structure, as opposed to their natural scattered pattern. A relatively simple way to achieve such a structure is by stretching the hydrogel unidirectionally such that the polymer chains align themselves in the direction of the applied force. Kim et al. employed such a strategy to develop an anisotropic double network hydrogel that exhibits similarly high mechanical properties to tendons. This was accomplished by developing a double network (DN) structure with alginate and polyacrylamide as the main polymers reinforced with silica microrods. This DN hydrogel was then stretched, dried, and crosslinked, as shown in Figure 2.10 below [68]. These DN hydrogels were also modified to exhibit impressive adhesive properties between tendon and bone through the incorporation of poly(2-hydroxyethyl aspartamide) modified with aminopropyl imidazole (PHEA-API) to form a triple network hydrogel [69].

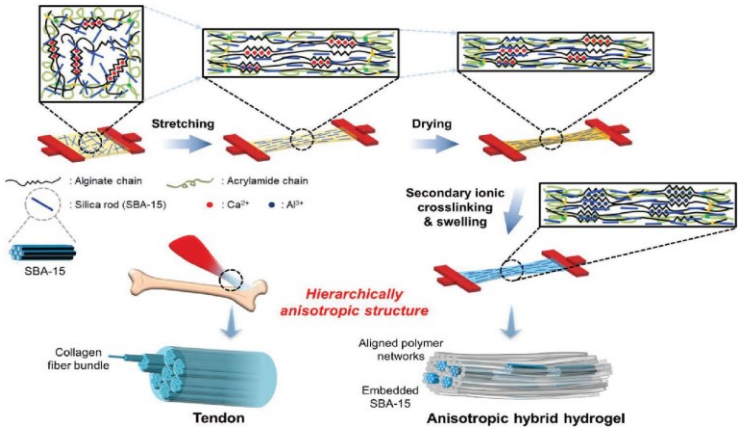

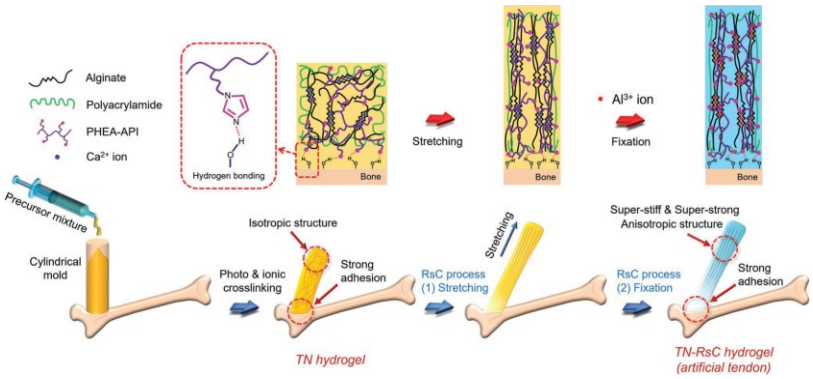

Figure 2.10: Design of the strong, stiff adhesive TN hydrogel. The TN, an energy-dissipative matrix, consists of three types of polymers: an ionically crosslinked Alg (Ca2+ ion; blue circle), covalently cross-linked PAM, and imidazole-containing adhesive polymers (PHEA-API). The final TN-RsC anisotropic hydrogel subjected to the RsC process (linear remodeling of polymers by stretching and fixation) was cross-linked by Al3+ ions and exhibited strong mechanical and adhesion properties [69]

While stretching hydrogels can align polymer chains to simulate anisotropic fibers, one of the key features of tendons and ligaments that contribute to their tensile properties is the hierarchical structure they possess. In this structure, thinner fibrils are collected into fibers, then those fibers into bundles, and this process continues until the full tendon and ligament is formed. Park and Kim mimicked this structure by braiding anisotropic hydrogel strands into a hierarchical hydrogel cable. These cables showed impressive load bearing capacities, being able to withstand heavy loads up to 13 kg and having a tensile strength of 4.7 MPa [72].

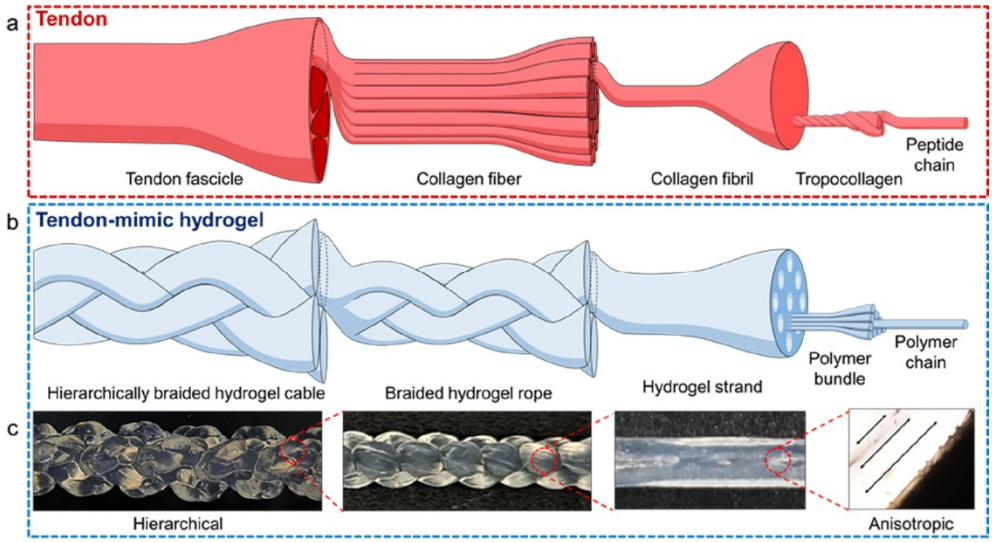

Figure 2.11: Schematics of a) tendon fascicle and b) its analogue, braided anisotropic hydrogel cable comprising anisotropic hydrogels. c) Photograph of the braided hydrogel cable, braided hydrogel rope, and anisotropic hydrogel strand and polarized optical microscopic image of a hydrogel strand showing an anisotropic structure [72].

Another technique that can be used to improve the physical performance of hydrogels is annealing. This process commonly involves heating up hydrogels beyond their crystallization temperature to increase the crystallinity of the polymer regions. These crystalline regions can act as obstacles to the propagation of tears in gels when they are stretched. Lin et al. proved this concept through the development of an anti-fatigue-fracture hydrogel that showed fatigue thresholds, defined as the critical energy released under loading, ranging from 110 J/m^2 without dry annealing to 1000 J/m^2 after 90 minutes of annealing [73]. In another approach, Wei et al. used solution annealing to develop chemically crosslinked cellulose gels, then proceeded to physically crosslink the gels through a solvent exchange using ethanol vapour [70]. Wu et al. combined these strategies and used solvent exchange and wet annealing to produce a strong hydrogel with anti-fatigue properties [71]. Under tensile stress, as would be experienced by tendons and ligaments in the body, these annealed hydrogels show significant resistance to tearing and maintain their physical properties over more cycles of mechanical loading. The solvent exchange method used by Wu et al. and Wei et al. also promotes entanglement amongst the amorphous polymer chains in the hydrogels. When stretched, these entanglements can be broken, and in doing so, energy is dissipated that provides strength to the hydrogel models.

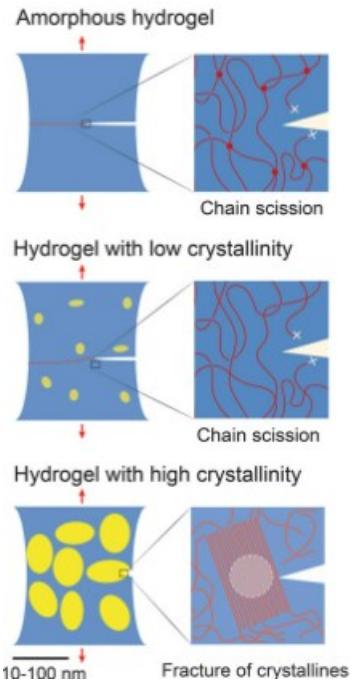

Figure 2.12: Illustration of fatigue crack propagation in an amorphous hydrogel and in hydrogels with low and high crystallinities under cyclic loads [73].

Cartilage

Cartilage exists on the caps of bones where it supports and protects the bone. While tendons and ligaments experience primarily tensile forces in the body, the main function of cartilage lies in its ability to resist compressive forces. When designing materials to mimic cartilage, many of the techniques and strategies used serve to improve or optimize the compressive and frictional properties of the material.

A common technique used in the design of cartilage mimicking materials is the creation of a double network (DN) hydrogel. Sometimes called interpenetrating network (IPN) hydrogels, these gels are developed by preparing a primary single network hydrogel, exposing it to a secondary network, and curing the two together. This process creates further crosslinking and greater entanglements which improve the hydrogels resistance to compression. This technique can many different types of polymers depending on the desired features for the hydrogel. Means et al. developed a cartilage mimicking hydrogel that had comparable modulus, strength, and lubricity to human cartilage. Means et al. combined poly(acrylamido-2-methylpropanesulfonic acid) (PAMPS) with poly(N-isopropylacrylamide) (NIPAAm) and acrylamide (AAm) to form a PMAPS/P(NIPAAm-co-AAm) DN hydrogel. Means et al. were able to achieve a compressive strength of approximately 25 MPa, a modulus above 1 Mpa, and a lower coefficient of friction than human cartilage. This was attributed to the anionic charges in the AMPS structure which contributed to a tightly crosslinked primary network, the stiffness of the NIPAAm component, and the hydrophilic nature of acrylamide which allowed the DN hydrogel to retain moisture more effectively [74]. Ding et al. used a multiphysical crosslinking approach to develop an IPN hydrogel that uses hydrogen bonds and ionic bonds to maintain its structural integrity while also carrying an equilibrium water content of over 70%. Acrylic acid (AA) and acrylamide (AAm) were the main components of the different networks, with xanthan gum (XG) and guar gum (GG) acting as sources of hydrogen bonding sites, and iron, Fe^{3+}, and tetraborate, $B_4O_7^{2-}$ acting as ionic crosslinking agents. The resultant hydrogels had an equilibrium water content of 72-76% and an elastic modulus between 1.4-3.3 MPa, which are comparable to the same properties in human cartilage [65].

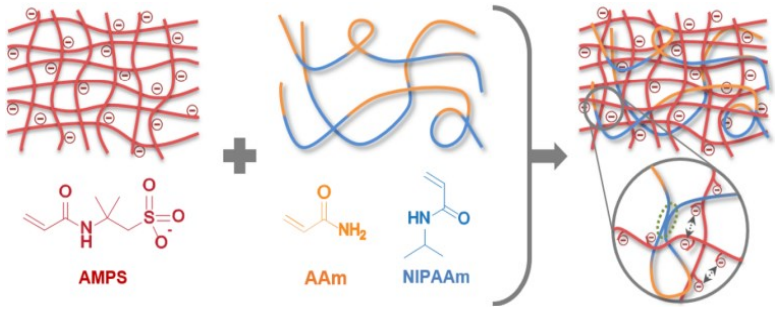

Figure 2.13: Illustration of Means et al.'s cartilage mimicking hydrogel [74].

Another technique used to mimic the structure of cartilage involves incorporating nanoparticles into hydrogels that provide stiffness and crystallinity to the gels. As the gels are compressed, one dimensional nanoparticles can apply opposing forces axially and as they break, they dissipate energy that further resists the compressive forces. Chen et al. used this principle to develop a bilayer hydrogel with a compressive strength of 5.21 ± 045 MPa, a compressive modulus of 4.06 ± 0.31 MPa, and hard-soft and soft-soft coefficients of friction of 0.032 and 0.028 respectively, all of which are comparable to human cartilage [66]. By using polydopamine (PDA) to form nanoparticles of Fe_3O_4 on a montmorillonite (MMT) surface, Chen et al. created magnetic PDA-Fe_3O_4-MMT nanohybrids that were then integrated into a polyvinyl alcohol and polyacrylic acid hydrogel. Then, upon inducing a magnetic field on the hydrogel, the nanoparticles aligned themselves in the direction of the magnetic field, effectively creating an anisotropic hydrogel. By using two different layers, one oriented perpendicular to the surface and one parallel, Chen et al. were able to better simulate the configuration of collagen fibers and chondrocytes in the cartilage [75]. Yu et al. employed a similarly layered approach by preparing a bilayer hydrogel, also known as a Janus hydrogel, that consisted of PVA, chitosan, sodium hyaluronate, with a hybridized, mineralized hydroxyapatite layer on the surface. The hydroxyapatite layer contributed to compressive strengths as high as 78 MPa while the negatively charged carboxyl groups on the surface of the hydrogel give the system a coefficient of friction of 0.024 [67].

Muscle

Muscles are a very important and complex group of tissues in the body that are responsive to various stimuli in the body, especially pH and electricity, contain anisotropic structures similar to the other tissues discussed, and possess impressive mechanical properties that enable them to support the body and facilitate locomotion.

It is believed that artificial muscles composed of multiple layers are capable of bending and straightening the arm in conjunction with the contraction of the biceps and triceps muscles. The simplest unimorphic system consists of a responsive layer and a non-responsive layer, referred to as active and passive layers, respectively. The sensitivity of a pH-responsive is based on its ability to associate and dissociate with hydrogen ions according to the pH of the aqueous environment. Using this concept, Ryan et al. developed an artificial muscle composed of a dry gel film, in which a strip of polyacid triblock copolymer was cast onto a glass microscope slide in an acetone/methanol solution[76]. Using tetrahydrofuran as the polybase, gel strips were cast and placed over the dried polyacid gel perpendicularly. The developed gel film can be bent in an acidic condition toward the anionic layer and in a neutral or basic condition toward the cationic layer (Figure 2.14) [76].

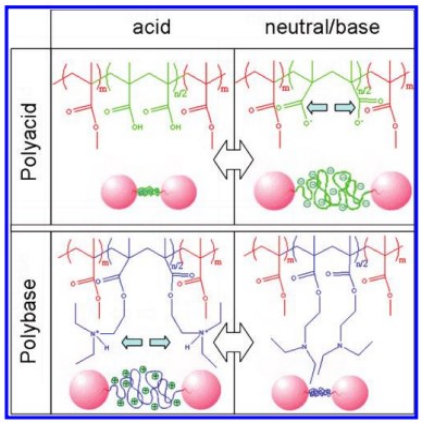

Figure 2.14: An illustration of the ionized and nonionized chemical structures and chain morphologies of the polyacid and polybase triblock copolymers under acidic and neutral/basic conditions. PMMA microdomains are represented by solid spheres [60].

A number of studies have also shown different strategies to make hydrogels that are responsive to electrical stimuli. Ismail et al. developed a composite hydrogel using electrically conductive polypyrrole and biocompatible chitosan polymers, to act as an artificial muscle in response to an electric current [60]. In electrolyte solutions as dilute as 0.01 M, the hydrogel actuator responded to electrical stimuli within five seconds, resembling the real mechanism that triggers natural muscle contractions. Bassil and coworkers followed this concept to design new electrobio-active hydrogel microfibers with high sensing and actuating capabilities [77]. As a result of the fabrication process, the microfibers possessed a tunable electroactivity with a 2D control of position at low driving voltages. The developed microfibers behave as well as or better than natural fibers. This solves complex problems related to advancing biomimetic mechanisms since the key is to develop sensors and actuators that behave like natural skeletal muscle. Inspired by previous studies, a smart and artificial muscle constructed of nanoparticles coated with ion-conducting nanoparticles was developed by Sun et al., whose work significantly improves ion conduction efficiency, mechanical properties, and electrochemical performance [78]. An anisotropic, highly conductive ion channel is then formed by intertwining it with MWCNTs and r-GOx (Figure 14).

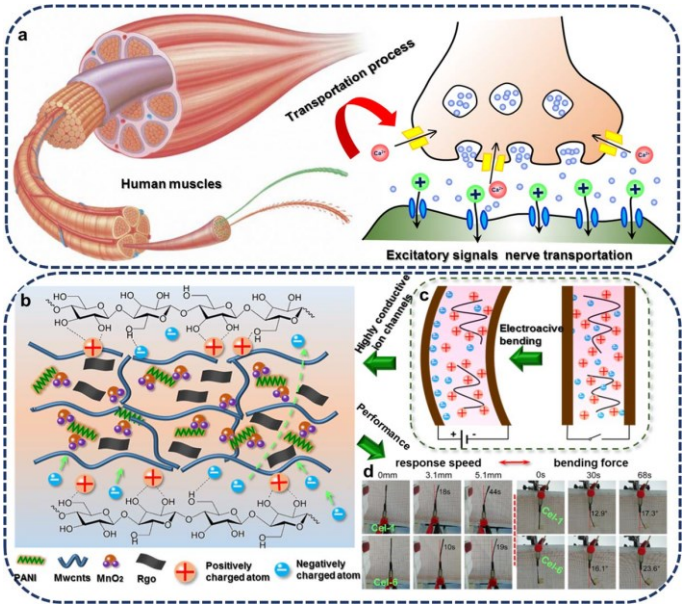

Figure 2.15: (a) Excitation transportation process of human muscle, (b) and (c) high-efficiency ion channel movement mechanism, and (d) electromechanical experiment of all-hydrogel artificial muscles [78].

With respect to anisotropy, it is possible to reproduce the unidirectional contraction and expansion of muscle fibers by amplifying the deformation of muscle-mimicking hydrogel in a specific direction (Figure 2.15). Sun et al. fabricated an anisotropic PEG-PNIPA hydrogel with an aligned dual network microstructure, exhibiting anisotropic two-dimensional shrinkage as a function of temperature [79]. The first network consists of an aligned porous PEG scaffold and the second network consists of PNIPA polymerizing within the pores. An aligned porous PEG scaffold is critical in achieving anisotropic shrinkage since it not only facilitates the formation of the PNIPA microcylinders but also constrains the axial shrinkage of cylindrical samples. The anisotropic PEG–PNIPA hydrogel has been demonstrated as an efficient and simple method of fluid regulation. In comparison with conventional hydrogels, anisotropic intelligent hydrogels offer advantages in terms of design and manufacturing.

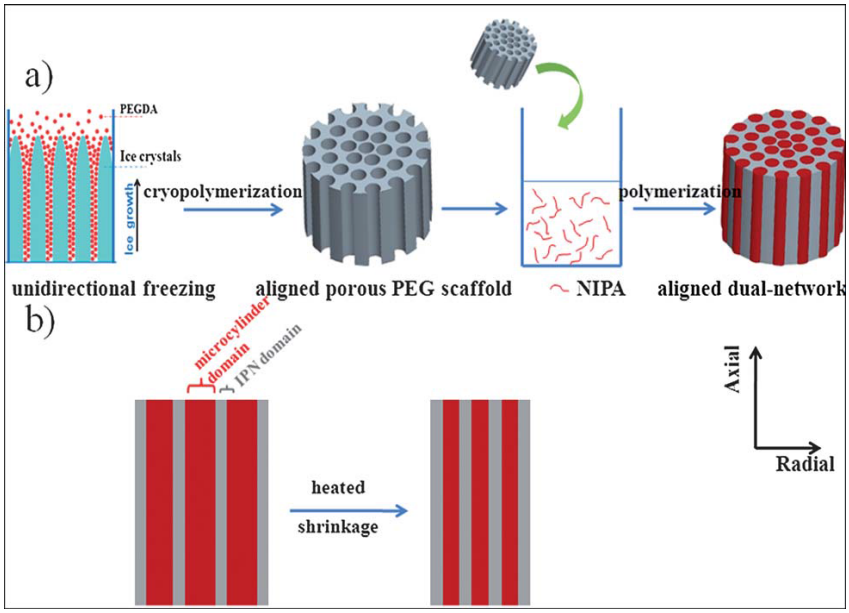

Figure 2.16: (a) Schematic illustration of the formation of the aligned dual network PEG–PNIPA hydrogel. (b) Proposed mechanism of the anisotropic shrinkage of the aligned dual-network PEG–PNIPA hydrogel [79].

There are a number of techniques for patterning, but 3D printing is one of the most promising. Wu et al. demonstrated the capability of 3D printing tough physical hydrogels that respond differently to programmed deformations. To print 3D objects using extrusion-based techniques, highly viscous solutions of poly(acrylic acid-co-acrylamide) (P(AAc-co-AAm)), poly(acrylic acid-co-N-isopropyl acrylamide) (P(AAc-co-NIPAm)), and/or their mixtures are used [61]. These mixtures are then submerged in a $FeCl_3$ solution where metal-coordination complexes work to crosslink the polymers. To achieve equilibrium, the gel constructs are submerged in a large quantity of water (Figure 2.17). The use of 3D printing in combination with structural control has enabled programmed deformations of hydrogels, known as 4D printing hydrogels. During the extrusion-based printing process, Lewis et al. incorporated stiff cellulose fibrils into NIPAm precursor solutions that were shear-oriented, resulting in nanocomposite gel fibers with anisotropic swelling properties [80]. By using 3D printing, such anisotropic gel fibers can be integrated into complex configurations and deformed in a controlled manner [81]. According to Zhao et al., the formation of tough double-network hydrogels is achieved by 3D printing physical alginate hydrogel, followed by polymerization to form the second network [81]. Additionally, tough physical hydrogel constructs can be created by printing salt-plasticized, polyion-complex solutions into water, where the gels were formed after removing the salt and forming ionic bonds between the polymers [62], [63].

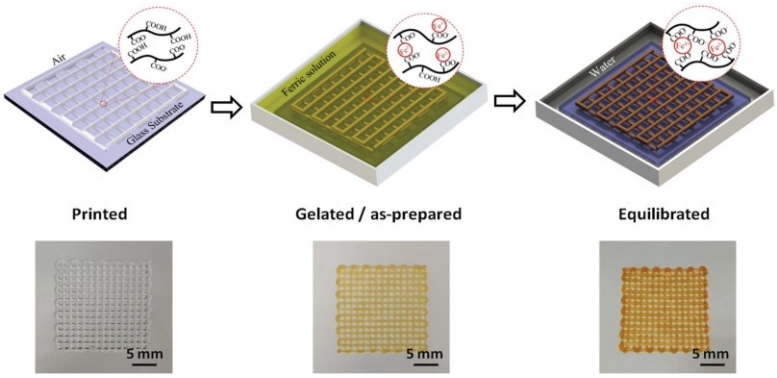

Figure 2.17: Fabrication of 3D-printed, tough hydrogels [61].

Living organisms use their muscles to actuate their body parts in order to perform various tasks. When picking up an object, the fingers should be bent to the appropriate degree and in the proper direction. Due to the anisotropic structure of certain hydrogels, which consist of parallel lamella networks, contraction of the polymer network results in bending of the hydrogel. Another approach relies on self-healing hydrogels, making the assembly of the hydrogel blocks into an integrated system possible. This results in composite motion of the integrated hydrogel. Yu et al. have developed a general, controllable strategy for constructing anisotropic nanocomposite hydrogels consisting of highly ordered lamellar precious-metal nanostructure assemblies (e.g. Ag, Au, Pt, and Cu). The hydrogels are fabricated by self-assembling metal nanostructures modified with thiolates as highly branched crosslinkers during in situ polymerization [64]. Silver nanoparticle/polyacrylamide (SNPP) hydrogels, as a typical example, exhibit exceptional anisotropic mechanical properties in addition to high strength. Through the interaction of the PAM network around lamellar silver assembly architectures, the tangent modulus parallel to the lamellae is 3.9 times greater than the tangent modulus perpendicular to the lamellae. There is also notable anisotropy in optics and swelling behaviour as well (Figure 2.18).

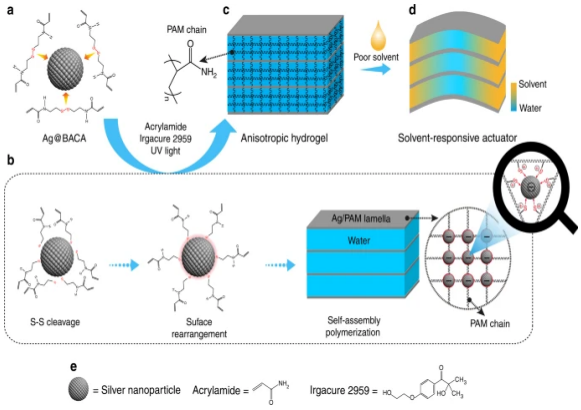

Figure 2.18: Illustration of how SNPP hydrogel is formed [64].

Skin

The largest organ in the human body, skin possesses anisotropic tensile, self-healing, and conductive properties that serve its role as a protective barrier between the rest of the body and the external environment. As the most superficial layer of the body, skin also plays a major role as a sensory organ for mechanical, thermal, and electrical stimuli. By selecting specific additives, these sensory capabilities can be imparted on hydrogels, allowing them to better replicate the function of skin in the body.

Taking inspiration from the structure of DNA, Q. Zhang et al. used a combination of adenosine monophosphate and quaternized chitosan (QCS) as additives to develop a polyacrylamide-based fatigue-resistant hydrogel with self-healing abilities and used sodium chloride in their design as a conducting agent. Stretching was used to make the resultant gel anisotropic, and under tension the QCS chains acted similarly to collagen in the body, contributing to the tensile strength of the material [55].

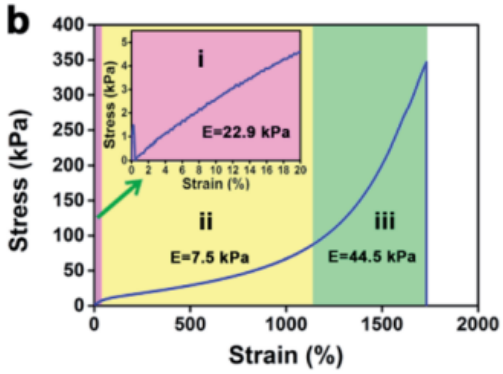

Figure 2.19: Stress strain curve for Q. Zhang et al.'s hydrogel model [55].

Polyacrylamide is a commonly used polymer in skin mimicking systems due to its mechanical strength along with its softness that is similar to human skin. Xia et al. also used polyacrylamide along with gold-polydopamine in a glycerol-base hydrogel and reported good adhesion to a number of substrates, high stretchability, and self-healing abilities [82]. In another instance of biomimicry, J. Zhang et al. copied Merkel cells, which act as mechanoreceptors in human skin, to develop an ionic hydrogel capacitive pressure sensor. This was done by combining collagen fibers with multi-walled carbon nanotubes and hydrolyzing the matrix in a NaOH and urea solution to create a 3D gel. The resultant gel contains pores to allow for the migration of ions throughout the network [83].

With respect to electronic sensing, conductive additives or wires can be incorporated into hydrogels to impart desired properties. Pan et al. used a proanthocyanin/reduced graphene oxide network in a PVA-borax hydrogel that was plasticized using glycerol [56]. D. Zhang et al. used a two-step method to fabricate cellulose biomimetic hydrogels, distributing a polyacrylamide

network throughout porous cellulose hydrogels. Their process resulted in a combination of collagen and elastin fibers in the hydrogel, which are the main components in human skin [57]. Yi et al. prepared a mold laden with ultrahigh molecular weight polyethylene (UHMWPE) fibers which provide a strain-limiting effect and impart an anisotropic property on the polyacrylamide gel [58]. Jo et al. took a similar approach, using a metallic nanowire as an electrode in a silk protein hydrogel [84]. These wires and fibers appear to be analogous to the Langer lines in human skin which dictate the anisotropic tensile properties of the skin. Taking a cue from the structure of plants, Yang and Yuan developed a zwitterionic biomimetic skin using cellulose nanocrystals (CNCs) as a filler in their hydrogel. The low density and significant hydrogen bonding capacity of CNCs enable them to act as a bridge throughout the hydrogel matrix, notably improving the mechanical properties of the hydrogel. Yang and Yuan reported a maximum tensile strength of 0.61 MPa as well as a maximum compressive strength of 7.5 MPa [59].

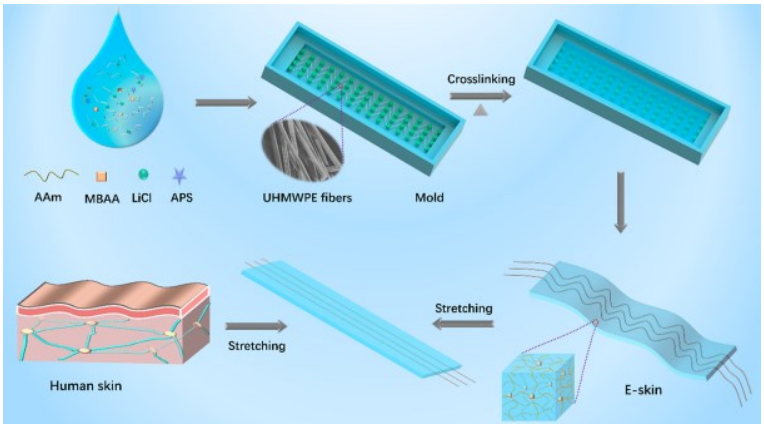

Figure 2.20: Yi et al's use of wires to mimic Langer Lines in a hydrogel model [58].

All of the skin-mimicking models discussed thus far have replicated skin using a single-layered approach. As mentioned earlier, human skin is a multilayered organ with the dermis providing the bulk of the mechanical properties due to its abundance of collagen and elastin fibers, and the epidermis providing significant barrier properties as the most superficial layer of the organ. Full-thickness, multi-layer skin models better represent the physiological structure of the skin while also possessing greater structural stability and improved barrier properties. [85] This makes the models more useful in applications such as surgical training models, cosmetics testing, and drug delivery where factors such as the thickness of the skin or diffusivity are important parameters.

Kwak et al. used gelatin methacrylate to construct a 3D hydrogel that represented the dermal and epidermal layers of the skin. To better replicate the structural properties of the skin, Kwak et al. incorporated fibroblasts into the dermal portion of the model and HaCaT keratinocytes into the epidermal section. By using a softer gelatin methacrylate matrix for the dermal portion and a stiffer matrix for the epidermal, the team was able to effectively replicate the layered structure of skin [86]. Wang et al. also used fibroblast and keratinocyte cells to accomplish a full thickness hydrogel

model, but instead opted for an interpenetrating polymer network as opposed to a layered model. This allowed for cells to better proliferate throughout the model by developing a dynamic network as opposed to a stubborn one. Wang et al. reported Young's moduli between 20-32 kPa and elongations at break of 50-70% [87].

Benefits & Drawbacks

Various types of hydrogels are utilized in tissue mimicking applications due to their softness and hydrated properties which resemble natural tissues. Both natural and synthetic hydrogel tissue-mimicking materials have been tailored to provide specific mechanical properties, controlled biodegradability, appropriate biochemical signaling, and architectural features that facilitate the mimicry of each component. However, the field also acknowledges certain drawbacks associated with hydrogels. Peppas & Khademhosseini shed light on the challenges and limitations of hydrogel-based approaches. Issues such as mechanical strength, and long-term stability pose significant hurdles in their widespread adoption, calling for innovative solutions and further research [88], [89]. Despite these challenges, hydrogels continue to hold promise in various biomedical applications. Annabi et al. discuss their potential as elastic sealants for surgical procedures, showcasing the versatility and adaptability of hydrogel-based materials in addressing clinical needs [90].

Some of the most pertinent mechanical properties of skin include its self-toughening abilities and its anisotropy. The tunable qualities of hydrogels provide an opportunity to better mimic these properties by manipulating the concentrations and selection of polymers that constitute the base gel as well as the crosslinking techniques that dictates the flexibility of the hydrogel. [55], [82] With respect to the anisotropic properties, the effects of additives including one-dimensional nanomaterials such as cellulose nanocrystals, or macro materials such as wires, are analogous to those of Langer lines [58], [84]. One significant drawback for existing hydrogel models of skin is the ability of the gels to maintain consistent performance under cyclic stress as skin experiences in vivo. Another is the tendency of hydrogels to lose moisture to the environment which jeopardizes the physical structure and mechanical properties of the hydrogels.

Similarly, the benefits of replicating cartilage using hydrogels lie in their tunable qualities. A number of studies have used a layering approach to effectively represent the gradient nature of the chondrocytes that provide articular cartilage with its mechanical properties [66], [67]. Current drawbacks for using hydrogels to replicate cartilage include the lack of data pertaining to: (i) the longevity of hydrogels *in vivo*, (ii) the fatigue resistance of the models, and (iii) the biocompatibility and bioactivity of the hydrogels. There is still a need for more research and

material development before hydrogels can be considered a viable candidate for in vivo cartilage replacement [91].

Hydrogels present significant benefits for mimicking muscle tissue, primarily due to their high water content, tunable mechanical properties, ability to form 3D structures, and biofunctionalization capabilities [92], [93]. Their resemblance to the hydrated environment of natural tissues makes them more similar to the environment in the body and conducive to cell encapsulation and proliferation [94]. Moreover, the mechanical properties of hydrogels can be adjusted to mimic those of native tissues by altering parameters such as polymer concentration and crosslinking density [93]. However, challenges exist in utilizing hydrogels for muscle mimicry. Their limited mechanical strength and stiffness compared to native tissues may compromise their ability to withstand physiological loads and maintain structural integrity over time [89]. Swelling and degradation in aqueous environments pose additional concerns, potentially altering mechanical properties and releasing degradation by-products [95]. The dense network structure of hydrogels could also impede nutrient and oxygen diffusion, impacting cell viability and tissue development. Furthermore, poor cell penetration into dense hydrogel networks may limit tissue integration, particularly in thick constructs or *in vivo* settings [96].

Moreover, hydrogels present promising prospects for tendon and ligament regeneration due to their biocompatibility, tunable mechanical properties, and ability to encapsulate cells and bioactive molecules [97]. They create a supportive environment for cell survival and tissue regeneration while offering the flexibility to match native tissue mechanics through adjustments in composition and crosslinking [98]. However, challenges such as limited mechanical strength, swelling, and diffusion restrictions must be addressed to ensure their long-term efficacy in tissue engineering applications [99]. Despite these drawbacks, ongoing research aims to optimize hydrogel design and functionality, unlocking their full potential in promoting the regeneration of functional tendon and ligament tissue.

Conclusion

Hydrogels are biomaterials with many potential applications in tissue mimicry and regenerative medicine. The literature highlights their benefits and drawbacks, shaping their role in mimicking muscles. In summary, each system of hydrogels—offers unique advantages and drawbacks for creating materials that mimic the mechanical properties of each component. The choice of method depends on specific application requirements, such as structural complexity, mechanical properties, and biocompatibility, and the intended use in tissue engineering and regenerative medicine. Hydrogels offer several advantages for creating materials that mimic the mechanical properties of muscles, including high water content, tunable mechanical properties, 3D structure,

and biofunctionalization capabilities. However, challenges such as limited mechanical strength, swelling and degradation, diffusion limitations, and poor cell penetration need to be addressed to optimize the performance and functionality of hydrogel-based scaffolds for tissue engineering and regenerative medicine applications. Additionally, while hydrogels offer significant promise for tissue engineering, addressing their inherent limitations is essential to harnessing their full potential in promoting tissue regeneration and functional recovery in these critical musculoskeletal structures. Continued research and innovation in hydrogel design and optimization hold the key to overcoming these challenges and advancing the field of tissue engineering.

3. Experimental Work

This chapter presents the experimental section of this thesis. Here, PVA hydrogels are modified using a solvent exchange with glycerol and thermal annealing to improve the compressive modulus and yield strength of the hydrogels. The results are presented, and key findings are identified and discussed.

The Effects of Solvent Exchange and Annealing on the Compressive Properties of PVA Hydrogels

Chukwunonso Moneme, Paula Wood-Adams

Abstract

In the world of tissue engineering, hydrogels are growing in popularity as a tissue mimicking material due to their tunability and softness. Many techniques have emerged over the years to improve the mechanical performance of these materials and allow them to more closely simulate biological tissues. One such technique, annealing, is commonly used to develop tough PVA hydrogels for tensile loading applications such as mimicking skin or muscle. This work explores the efficacy of thermal annealing and solvent exchange in the development of hydrogels intended for compressive loading applications such as mimicking cartilage. Hydrogels were prepared using an adapted double solvent exchange method, and underwent compressive testing after being annealed for 0, 30, 60, 90, and 120 minutes. FTIR and DSC were used to investigate the thermal and chemical behaviour of the hydrogels in different stages of development. The FTIR results showed evidence of conformational changes in the hydrogel throughout development, as well as a lack of chemical reactions. The DSC results contained evidence of plasticization due to residual glycerol from the solvent exchange processes. The resultant hydrogels possessed increased compressive moduli and yield strengths with increased annealing time up to a peak time of 90 minutes.

Introduction

Hydrogels are a class of material of interest in the domain of tissue engineering as potential candidates for the simulation of biological tissues. At its most basic, a hydrogel is a network of polymeric material dispersed through an aqueous matrix. Hydrogels are soft, customizable, and highly tunable, which makes them attractive candidates in tissue engineering where mimicking each type of tissue may require different properties. In their most simple state, however, hydrogels do not tend to possess the mechanical strength or resilience necessary to simulate biological tissues which regularly undergo repetitive mechanical stresses. To overcome this, a number of techniques and strategies have been developed over the years to strengthen and toughen hydrogels. Some examples of these include combining different types of polymers into one hydrogel, producing double network or interpenetrating network hydrogels, twisting and braiding hydrogels together to mimic the structure of muscles, and using additives to promote greater crosslinking, or otherwise manipulate the properties of the gel.

One technique that is quite simple in both concept and execution is annealing. This involves heating up a hydrogel beyond the crystallization temperature of the polymer to condense the polymer molecules and facilitate increased crystallization. This increased crystallization bolsters the mechanical properties of the polymer. This technique is quite extensively used in tensile applications, which are very important when simulating tissues such as skin, muscle, tendons, or ligaments. There are, however, tissues such as cartilage which do not undergo tensile stresses as much as they do compressive loads. Much of the literature around annealing of hydrogels explains the impacts of crystallization in the context of stretching and tearing. Lin et al. even uses annealing to develop anti-fatigue-fracture hydrogels that can “maintain robustness under cyclic mechanical loads” within the context of tensile loading [73]. There is, however, a lack of data in the literature about the efficacy of thermal annealing as a technique in developing strong hydrogels to undergo compressive loading. An important limitation of annealing, though, is that it requires relatively high temperatures, around or exceeding 100 °C. Given the vaporization temperature of water, annealing thick hydrogels can result in a loss of volume that is not easily restored. There has been recent research, however, on a wet annealing process to produce hydrogels that could circumvent that issue entirely [71]. This technique employs solvent exchange processes and combines it with thermal annealing to produce mechanically strong hydrogels. This work aims to explore if such a process could be effective in producing hydrogels intended to undergo compressive loading. This will allow for the evaluation of the utility of this technique in the development of hydrogels intended to simulate tissues such as articular cartilage in the human body.

Methodology

Developing Hydrogels

First, 15 wt.% of neat PVA (from Sigma-Aldrich, Mw 85 - 124 kg/mol, >99% hydrolyzed) was added to a beaker with a stir bar, followed by distilled water. The beaker was then covered to minimize evaporation and placed on a stirring hot plate at 160 °C and 400 rpm. Mixing was continued for 3 hours, then the speed and temperature were both turned down to allow bubbles to move to the surface of the mixture. Small volumes, of ~ 5 mL, were placed in the freezer overnight at -20 °C. Afterwards, the gels were allowed to thaw at room temperature for 2 hours. The hydrogels were placed in an excess of glycerol for 48 hours to allow for solvent exchange. The resultant organogels were then annealed in a furnace at 100 °C for times ranging from 0 to 120 minutes. After annealing, the gels were submerged in water for 48 hours to finish the second solvent exchange and once again produce hydrogels.

To facilitate discussion, the gels will be referred to as the “initial hydrogel” after they have been freeze-thawed but before further modification, “organogel” after undergoing the first solvent exchange to glycerol, and “rehydrated” after the second solvent exchange back to water. Different annealing times will be indicated by “unannealed” for 0 minutes and 30, 60, 90, or 120 min accordingly for the rest.

Fourier-Transform Infrared Spectroscopy

Fourier-transform infrared spectroscopy (FTIR) was used to investigate the bonds present in the hydrogels throughout their development. The FTIR tests were conducted at wavelengths ranging from 500 – 4000 nm. Each sample was tested in three different locations and the intensities of each test were averaged to obtain the curves for each specimen.

Differential Scanning Calorimetry

Differential scanning calorimetry (DSC) was used to investigate changes in the crystallinity and thermal behaviour of the hydrogels throughout their development. The DSC was conducted from 25 – 250 °C at a heating/cooling rate of 5 °C/min on a heat-cool-heat cycle. The cooling and second heating peaks of each of the curves were analyzed using the TA Universal Analysis software. The first heating curves were omitted due to inconsistencies in the shapes and numbers of peaks. Each test was performed in triplicate, and the values obtained from the peak analyses were averaged. One-way ANOVA analysis with a Tukey post-hoc test was conducted for the melting and crystallization peaks after different annealing times.

Compression Testing

Compression tests were conducted on a Universal Testing Machine (UTM) from Hoskin Scientific using a 5000 N load cell. The gel samples used were discs and the diameter and thickness of each disc were measured using a calliper. The data obtained was modified to present strain as a percentage (ε) of the initial length (L_0), and stress (σ) in Pascals from the recorded force (F) and the initial cross-section area (A). Each sample was subjected to 8 replicates due to a significant variation in the data. Outlier analysis was conducted, and the results of the compressive modulus and yield strength after different annealing times were put through a one-way ANOVA analysis with a Tukey post-hoc test.

The curves obtained were viewed on a double logarithmic scale to determine the periods of linearity at the beginning of each curve. A strain range of 0.5-5% was identified as the linear region for all specimens, and linear regression was used to obtain the slope, taken to be the compressive modulus of each unique specimen. To identify the yield strength, the linear model was extrapolated along the full range of each curve. The standardized residuals (r_i) were then calculated from the real residuals (e_i) between the linear model and the actual stress, and the mean of the residuals ($\bar{e}$) as shown in Equation 1 [100]. The point at which the residuals for each curve began to consistently exceed 0.0002 was selected as the yield point, representing the onset of plastic deformation.

$$r_i = \frac{e_i}{\sqrt{\frac{1}{n-1}\sum_{i=1}^{i=n}(e_i - \bar{e})^2}} \tag{1}$$

Results

Hydrogel Development

To circumvent the issue of water evaporation, a modified version of the solvent exchange method performed by Wu et al. was employed to allow the annealing to take place without significant loss of thickness [71] After solvent exchange the organogels were detectably 18% smaller in diameter ($p<0.001$) and 24% in thickness ($p<0.001$) and they were also tangibly stiffer. The gels softened and returned to almost their initial size after being submerged in water for 48 hours.

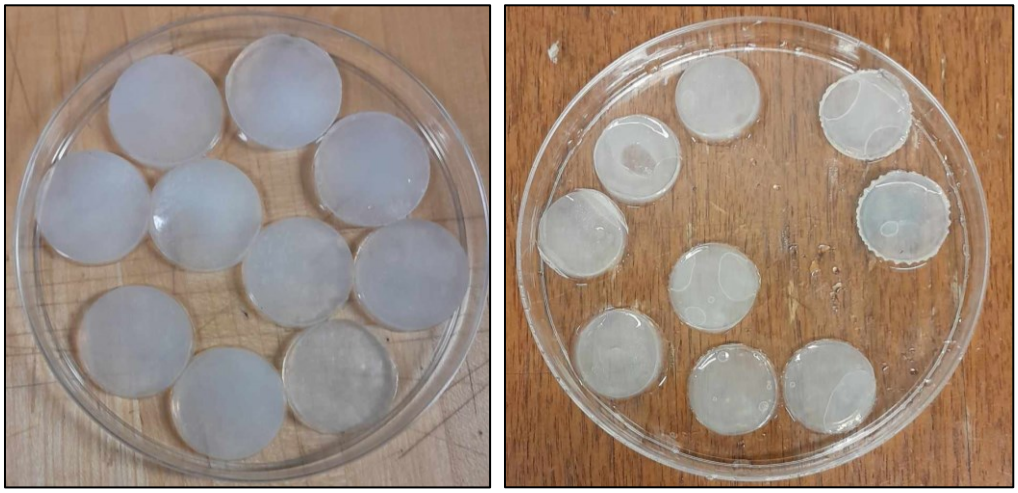

Figure 3.21: Hydrogels after being frozen and thawed (left) and organogels after the solvent exchange to glycerol (right).

FTIR

A comparison of the FTIR spectra for the materials used in developing the hydrogel, as well as the spectrum for one annealed and rehydrated hydrogel sample, is displayed in Figure 3.2 below. The PVA spectrum contains a broad band at 3300 cm^{-1} attributed to hydrogen bonding and -OH vibrations. Due to the significant presence of OH groups in the structure of both water and glycerol, this broad band is present in all spectra. The peak located at around 2880 cm^{-1} is assigned to CH bonds as are the peaks at around 1430 cm^{-1}, and the peak located at 2930 cm^{-1} is assigned to CH_2 bonds [101]. Other than the 3300 cm^{-1} OH band, the neat water spectrum only contains one other band at around 1700 cm^{-1}. While bands in this region are commonly associated with carbonyl groups, here this band actually represents the H-O-H bending resonance of water [102]. Lastly, the glycerol spectrum contains the OH peak at 3300 cm^{-1}, CH_2 and C-O-H stretches overlapping between 1210 and 1420 cm^{-1}, and most uniquely, a series of C-O stretches representing primary and secondary alcohols between 990 and 1110 cm^{-1} [103]. The final spectrum of the annealed and rehydrated hydrogel displays a combination of bands from the three components' spectra, especially PVA and water.

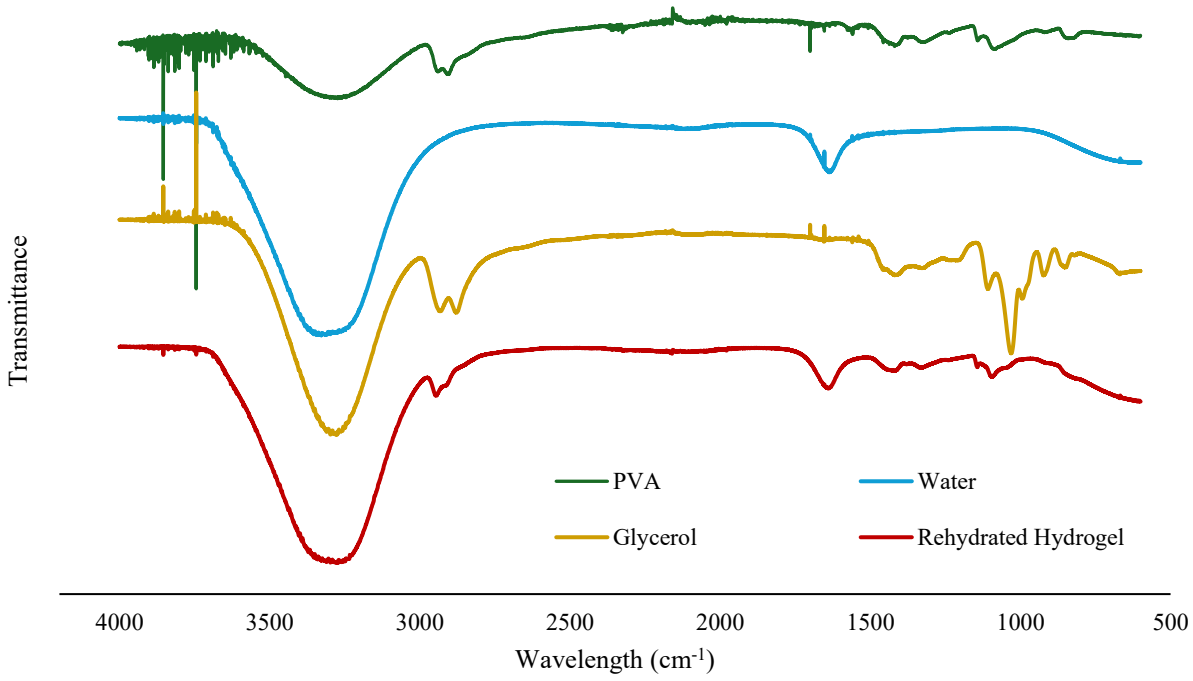

Figure 22: Comparison of the FTIR spectra of the hydrogel components.

Figure 3.3a below compares the FTIR spectra of the gels at different stages in the process. From top to bottom the spectra represented are of the hydrogel after being frozen and thawed, then the organogel after the first solvent exchange, the same organogel after being annealed for 60 min, and

lastly the rehydrated hydrogel. Comparing the bands of the initial hydrogel and organogel spectra, the notable reduction in the HOH peak of water at around 1700 cm^{-1} combined with the amplification of the CH_2 and CH peaks at around 2900 cm^{-1} and the introduction of the alcohol peaks at around 1000 cm^{-1} indicate that the solvent exchange from water to glycerol occurred as expected. When the organogel is annealed, the HOH peak almost entirely disappears, and the CH and alcohol peaks are further amplified. This indicates that residual water is evaporated during annealing. Upon rehydrating the annealed gel, the spectrum returns to a form similar to the initial hydrated spectrum.

The amplitudes of the PVA associated peaks of the rehydrated gel fall between that of the initial hydrogel and those of the organogels, as shown in Figure 3.3b below. Specifically, the rehydrated spectrum shows amplifications in the CH_2 and CO peaks at 2935-2950 cm^{-1} and 1090-1100 cm^{-1}, respectively, as compared to that the initial hydrogel. This indicates that the conformation of the PVA network chains in the organogel is partially preserved in the rehydrated sample. The shoulder in the rehydrated spectrum at 1046 cm^{-1} indicates that a small amount of glycerol remains in the hydrogel matrix after rehydration. The lack of new peaks throughout the process suggests that no chemical changes are occurring.

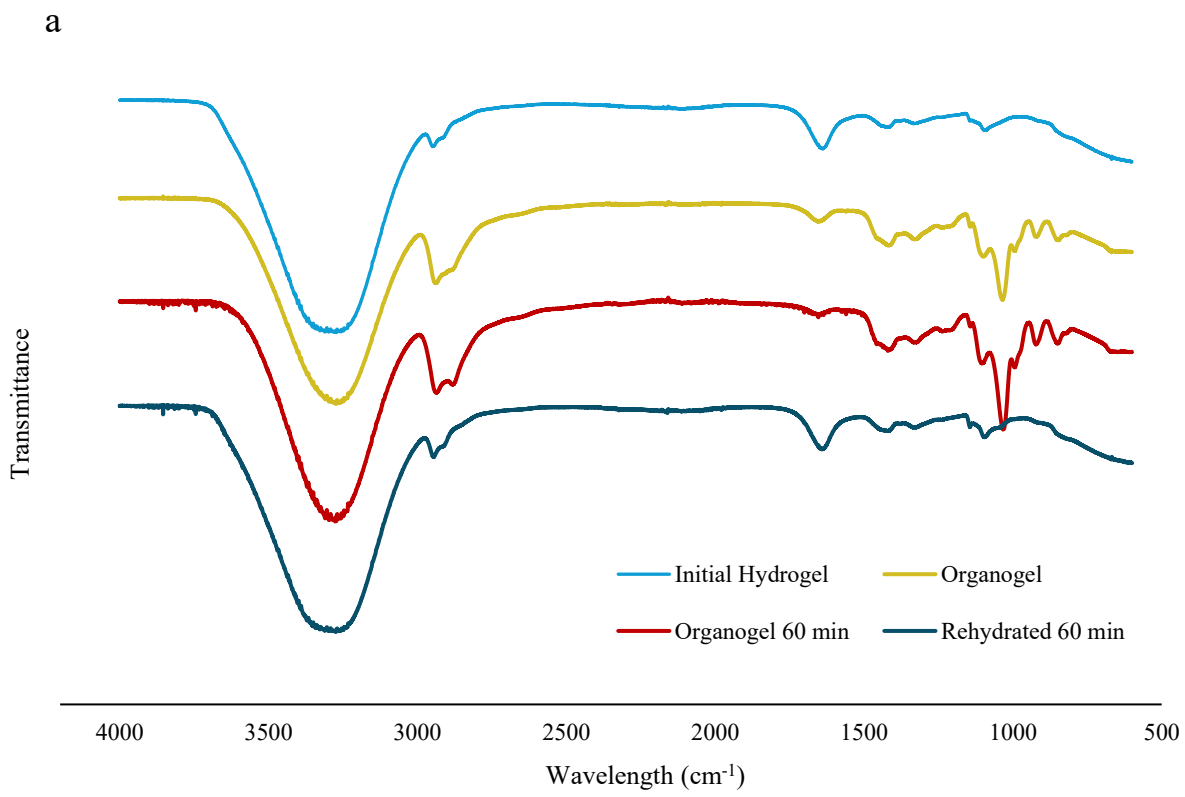

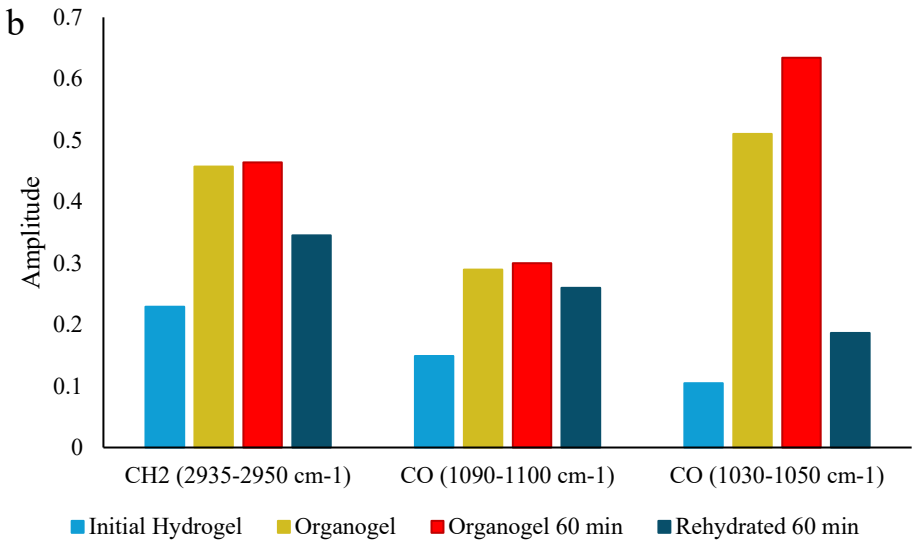

Figure 3.3: (a) Comparison of the FTIR spectra for the hydrogel at different stages of development. (b) Amplitudes of CH_2, and CO peaks for each spectrum.

Figure 3.4 below contains the FTIR spectra for each of the organogels and rehydrated gels after 30, 60, 90, and 120 minutes of annealing. Annealing time has no significant effect for either the organogels or hydrogels. There is, however, a notable difference in the spectrum between the unannealed organogel and the annealed organogels. This is believed to indicate a conformational change of the PVA network that occurs during annealing for at least 30 min.

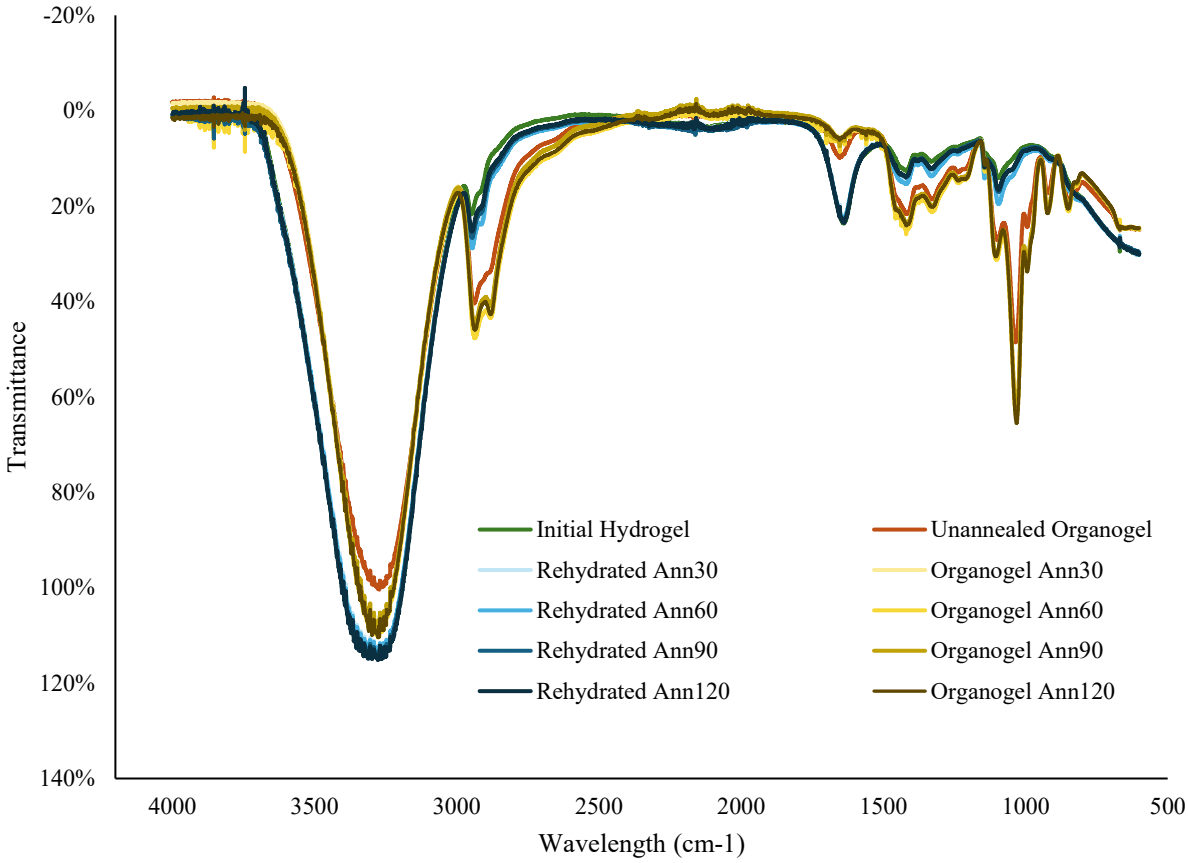

Figure 23: FTIR Spectra of organogels and hydrogels after annealing at different times

DSC

Figure 3.5 below shows the DSC thermograms of two series of hydrogels. The first series is the initial hydrogel that is simply PVA solubilized in water, frozen, thawed and annealed (in water) for varying times. The second series is the hydrogel which underwent solvent exchange to glycerol prior to annealing in glycerol, and then rehydration in a second solvent exchange process. In Figure 3.5b we observe a notable shift in both the melting and crystalline peaks as annealing time increases, while no such shift is observed in Figure 3.5a with the peaks overlapping quite neatly. Since the only difference in the samples tested is the solvent exchange with glycerol, it stands to reason that this shift is a result of some interaction between the hydrogel structure and glycerol.

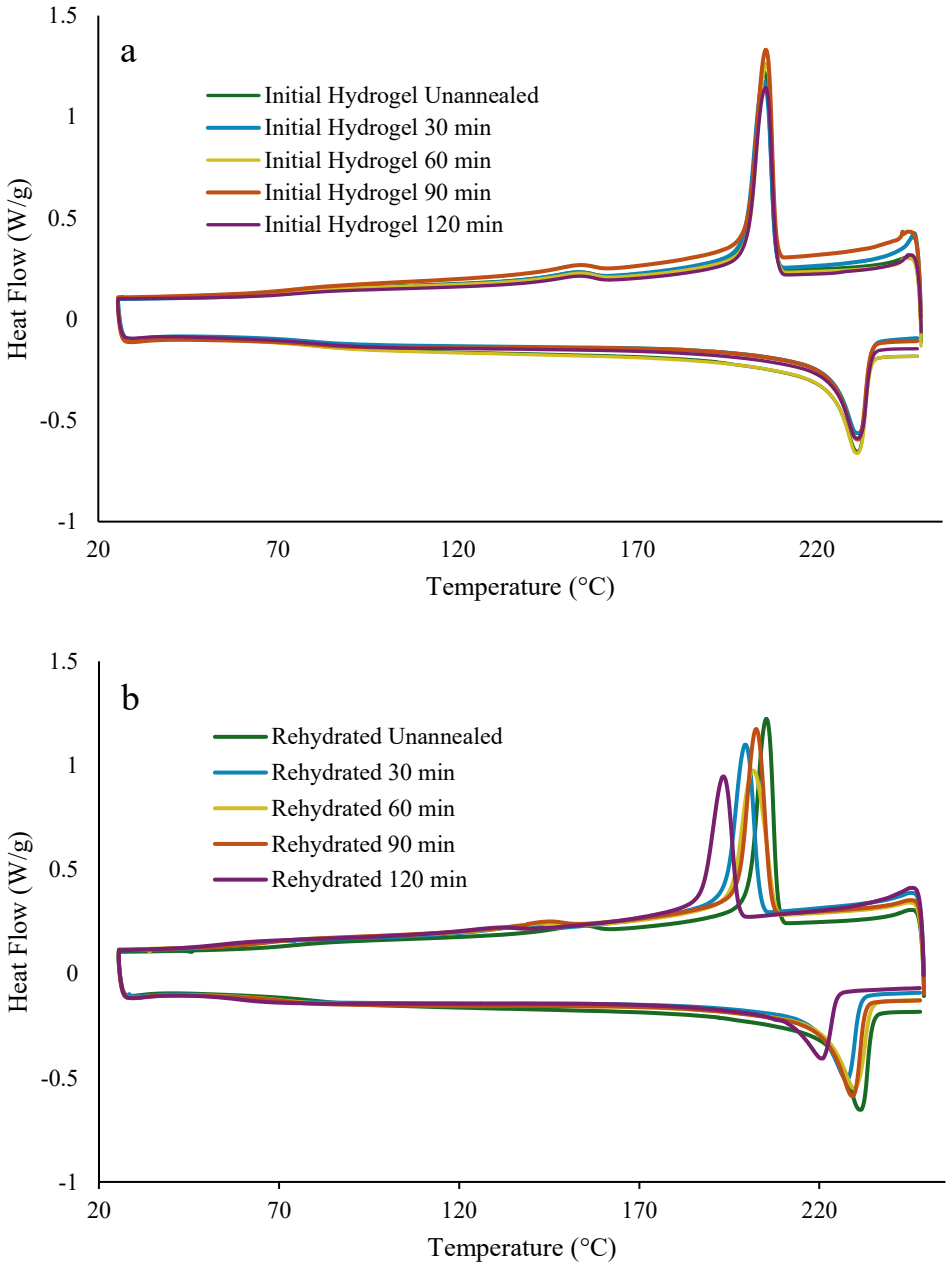

Figure 24: DSC thermograms of (a) initial hydrogels and (b) rehydrated hydrogels.

In Figure 3.6, we see a minimum crystallization temperature after 90 minutes of annealing. However, the one-way ANOVA test also indicates a lack of statistical dependence on annealing time, with high p-values ($p>0.05$) for the melting and crystallization peak temperatures.

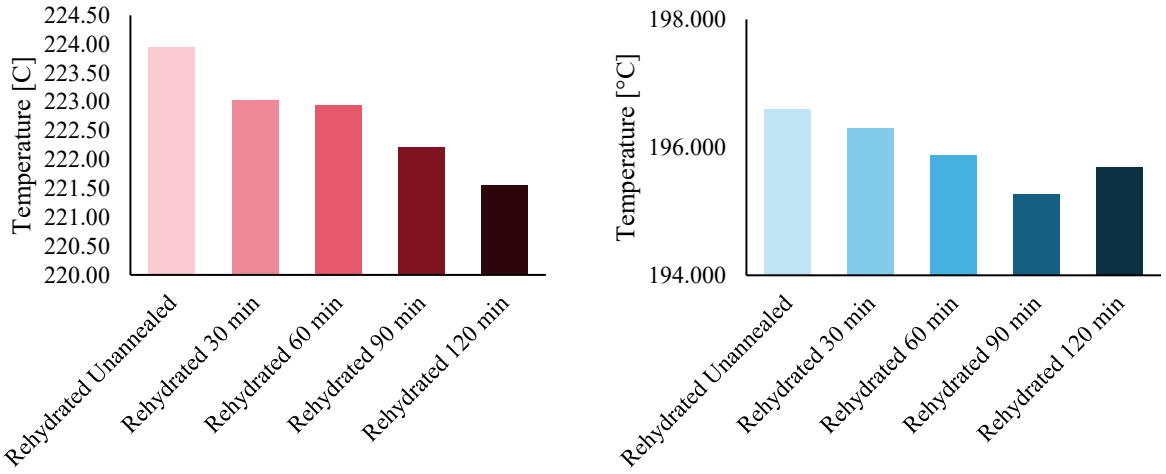

Figure 25: Graphs showing the peak temperatures for the melting (endotherms) and crystallization (exotherms) peaks. Data included is the average of 3 repeats per specimen.

Compression

The compression test results across different annealing times shows similar trends in the compressive modulus and yield strength of the hydrogels. There was a steady increase in both modulus and yield strength ($p = 0.015$ and 0.001, respectively). Pairwise post-hoc comparison indicated that it took 90 minutes of annealing for modulus ($p = 0.021$) and yield strength ($p = 0.001$) of the PVA to detectably increase.

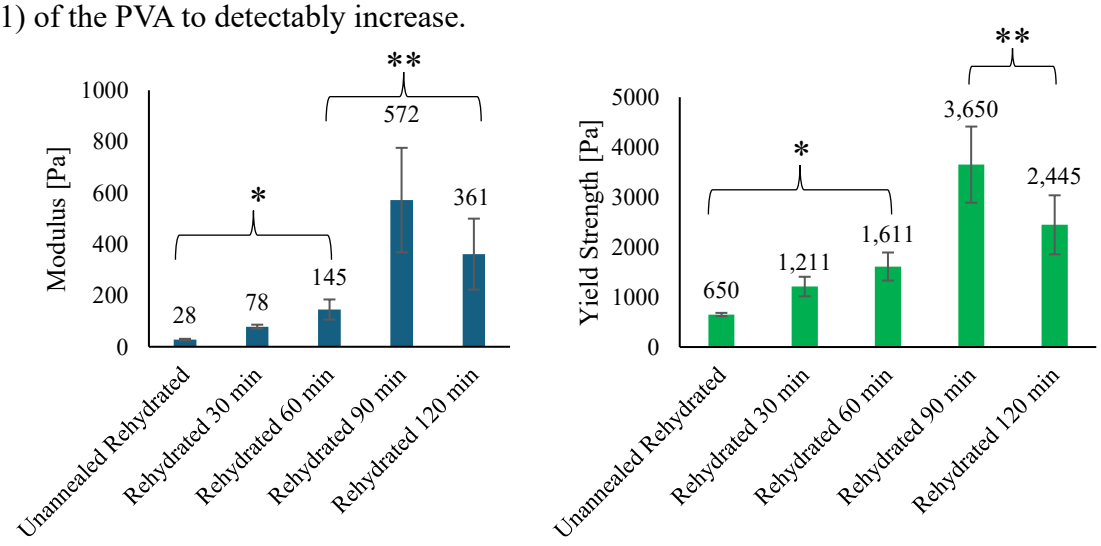

Figure 26: The compressive modulus and yield strength of rehydrated hydrogels with different annealing times. Data points are the mean of 8 repeats per specimen, with bars indicating standard error. P-values for the compressive modulus and yield strength are 0.015 and 0.001 respectively. Homogeneous subsets are indicated with asterisks (, **).*

Comparing the compressive properties of the hydrated samples to the organogels, there is a significant difference between their values. While the hydrogel samples had a maximum modulus

and strength of approximately 572 and 3650 Pa respectively, the organogel samples had maximum values of approximately 1880 and 7000 Pa respectively. There was also a considerable increase in both properties of the organogels after annealing.

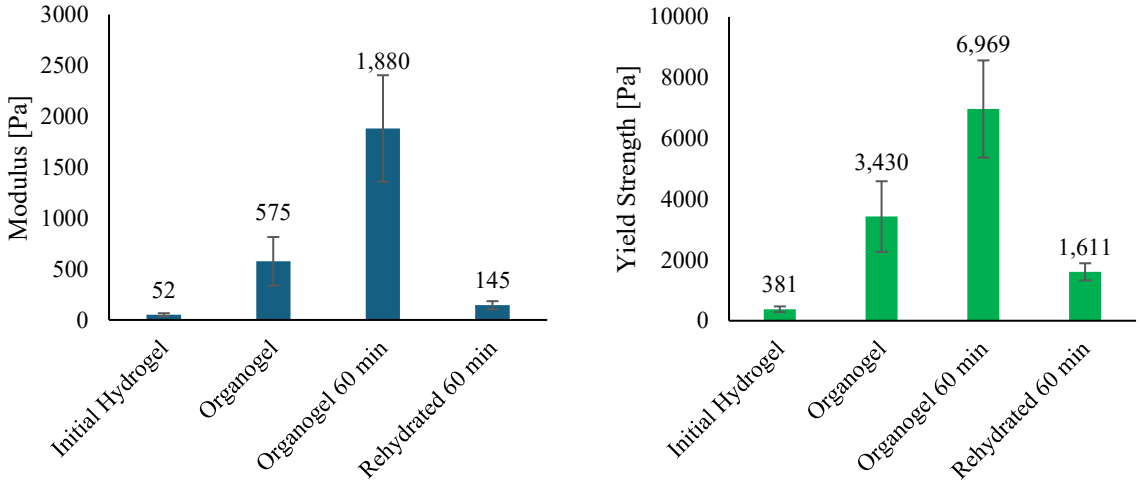

Figure 27: The compressive modulus and yield strength of hydrogels at different stages of the process. Data points are the mean of 8 repeats per specimen, with bars indicating standard error.

Comparing the initial hydrogel to the rehydrated hydrogel after both solvent exchange steps, but without annealing in between, there is a reduction in the compressive moduli of the gels. The rehydrated hydrogel in this case had a compressive modulus of 28 Pa while the initial hydrogel had a modulus almost twice that at 52 Pa, as shown in Figure 3.9 below.

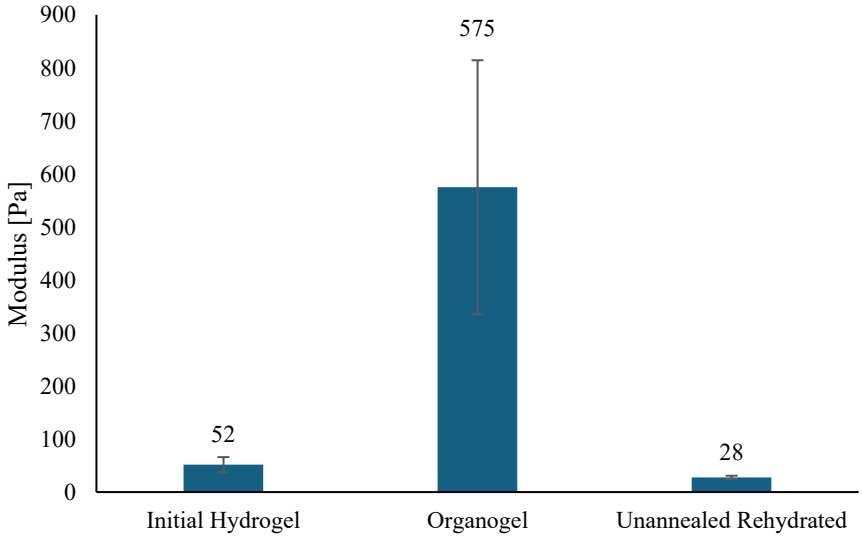

Figure 28: The compressive modulus of the initial and rehydrated unannealed hydrogels, as well as the unannealed organogel. Data points are the mean of 8 repeats per specimen, with bars indicating standard error.

Discussion

The double solvent exchange method of hydrogel production process outlined in this work makes use of two distinct mechanisms. One is thermal annealing, and the second is the solvent exchange with glycerol.

The compression test results confirm that thermal annealing does increase the compressive modulus and yield strength of the hydrogels, with a significant improvement at around 90 minutes of annealing. The fact that the samples that were annealed for 90 minutes outperformed the samples that were annealed for 120 minutes is in line with similar tensile tests performed by Wu et al. [71]. This result implies that the annealing time can be optimized depending on the components and properties of the desired hydrogel. The FTIR results also suggest that these differences in mechanical properties are not due to any chemical differences in the makeup of the hydrogel components, meaning that the introduction of glycerol did not produce byproducts or molecular changes in the hydrogel matrix. The differences in the FTIR spectra for the initial and rehydrated hydrogel suggest that the hydrogel underwent conformational changes throughout its development, and that a small amount of glycerol remained in the hydrogel matrix after the second solvent exchange back to water. Glycerol has been reported to have a plasticizing effect in PVA networks and has also been reported to lower the melting and crystallization temperatures of the polymer [104], [105]. Since plasticizers increase the mobility of polymer molecules, the presence of glycerol in the system should correspond with a reduction in the modulus of the hydrogel. This is observed in the compression data as seen in Figure 3.9, which shows that when the hydrogel undergoes a solvent exchange to glycerol and another back to water with no annealing in between, the compressive modulus decreases by almost 50%, from 52 Pa to about 28 Pa.

While the presence of trace amounts of glycerol in the hydrogel matrix reduces the compressive modulus of the hydrogel, the organogel possesses a modulus almost double that of the hydrogel after rehydration. This can be attributed to the compacting of the PVA chains that occurs in glycerol due to its nature as a poor solvent for PVA [71]. This densification of the hydrogel reduces the distance between PVA molecules which can be seen in the change in the physical dimensions of the gel after it was soaked in glycerol. This compacting of the polymer chains allows the interactions between the PVA molecules to overcome the interactions between PVA and glycerol, which facilitates greater crosslinking through crystallization. As the gels are annealed, changes occur in the conformations of the amorphous segments of PVA, which forms a stronger 3-dimensional network. This results in an impressive modulus of 1880 Pa before the second solvent exchange back to water, which is also a significant change from a modulus of about 575 Pa in the organogel before annealing. The FTIR results in Figures 3.3b and 3.4 indicate that the conformational effect of glycerol and annealing is at least partially retained after the second solvent exchange to water due to the physical crosslinking. This ultimately results in the improved mechanical properties of the rehydrated annealed samples as compared to those of the rehydrated unannealed samples as seen in Figures 3.7 and 3.8.

Conclusions

Based on the results presented, it is apparent that thermal annealing in glycerol can be an effective strategy for producing hydrogels with improved compressive mechanical properties in addition to tensile properties. The issue of losing volume in the hydrogel due to the evaporation of water at high temperatures is also avoided through the solvent exchange process. Solvent exchange, with a poor solvent for the polymer, as glycerol is for PVA, further promotes crystallization and produces a stronger 3-dimensional hydrogel. While the solvent exchange facilitated a more effective annealing process and greater crystallization in the PVA hydrogel matrix, the double solvent exchange process does not improve the mechanical properties of the hydrogel without thermal annealing. Similarly, thermal annealing without the solvent exchange results in highly compacted hydrogels due to the evaporation of water which provides the hydrogel with its volume. It is also important to note that the DSC and FTIR both showed evidence of residual glycerol remaining in the rehydrated gel matrix. Though the impact this had on the mechanical properties was not particularly significant, it is important to take note of, especially if the hydrogel were to be used in *in vivo* applications. While the hydrogel showed improved mechanical properties, the organogel showed the best mechanical properties due to the densification of the PVA network. This suggests that other toughening strategies such as double network gels may be more effective techniques in developing hydrogels for compressive loading applications depending on the desired mechanical properties [106], [107].

4. Conclusion & Future Work

This work explored the utility and potential of hydrogels in tissue engineering applications. Chapter 2 outlined many developments that have emerged in recent years which improve the mechanical properties of hydrogels and allow them to mimic other functions of biological tissues such as self-healing, conduction, and stimuli-response. There is still work to do to address the limitations that are inherent to hydrogels, especially their mechanical strength, swelling and degradation behaviour, and diffusion limitations. Addressing these challenges could unlock a greater range of applications in tissue replacement and regeneration. Chapter 3 looked specifically at the development of hydrogels for compressive loading, which are relevant in mimicking tissues such as cartilage. Ultimately, this study demonstrated that thermal annealing can be an effective strategy for the development of hydrogels with improved compressive mechanical properties. While standard annealing would evaporate the water in the hydrogel matrix, the solvent exchange method not only maintained the volume of the hydrogels, but also densified the gel, facilitating more extensive crosslinking during annealing. The combination of these two techniques resulted in notably improved compressive mechanical properties.

4.1. Future Work

The research outlined in Chapter 3 would be well complemented with some further development and experimentation that could not be included in this work due to resource limitations. First, a more thorough investigation into the optimization of the hydrogel network by using different concentrations of PVA and glycerol could provide more information about the interactions between the components and the extent of the impact that the solvent exchange can have on the mechanical performance of the hydrogel. Moreover, conducting fatigue testing on the developed hydrogel could provide deeper insights into the longevity of the hydrogel and the consistency of the improved mechanical properties under continuous cyclical compressive loading. Lastly, while the method explored in Chapter 3 produced tougher hydrogels, the maximum compressive modulus and yield strength were 572 and 3650 Pa respectively. These are both significantly lower than the same values of biological cartilage, 0.5-1 and 10 MPa respectively, as identified in Chapter 2. To achieve these values, incorporating an interpenetrating network approach with the solvent exchange and annealing could be a viable approach. Combining these techniques would further densify the system and increase the crystallization, both of which would improve the mechanical properties of the hydrogels system.

References

[1] A. Ostadfar, “Tissue Engineering of Cardiovascular System,” in *Biofluid Mechanics*, Elsevier, 2016, pp. 323–339. doi: 10.1016/B978-0-12-802408-9.00009-0.

[2] A. K. Dąbrowska *et al.*, “Materials used to simulate physical properties of human skin,” *Skin Research and Technology*, vol. 22, no. 1, pp. 3–14, Feb. 2016, doi: 10.1111/srt.12235.

[3] F. Xu *et al.*, “Hydrogels for Tissue Engineering: Addressing Key Design Needs Toward Clinical Translation,” *Front Bioeng Biotechnol*, vol. 10, May 2022, doi: 10.3389/fbioe.2022.849831.

[4] “Hip and Knee Replacements in Canada: CJRR Annual Report, 2021–2022,” Ottawa, 2023.

[5] H. Hsu and R. M. Siwiec, *Knee Osteoarthritis*. 2024.

[6] H. Yousef, M. Alhajj, A. O. Fakoya, and S. Sharma, *Anatomy, Skin (Integument), Epidermis*. 2024.

[7] T. M. Brown and K. Krishnamurthy, *Histology, Dermis*. 2024.

[8] W. D. Losquadro, “Anatomy of the Skin and the Pathogenesis of Nonmelanoma Skin Cancer,” *Facial Plast Surg Clin North Am*, vol. 25, no. 3, pp. 283–289, Aug. 2017, doi: 10.1016/j.fsc.2017.03.001.

[9] K.-M. Lim, “Skin Epidermis and Barrier Function,” *Int J Mol Sci*, vol. 22, no. 6, p. 3035, Mar. 2021, doi: 10.3390/ijms22063035.

[10] K. A and L. A, “Mechanical Behaviour of Skin: A Review,” *Journal of Material Science & Engineering*, vol. 5, no. 4, 2016, doi: 10.4172/2169-0022.1000254.

[11] W. Yang *et al.*, “On the tear resistance of skin,” *Nat Commun*, vol. 6, no. 1, p. 6649, Mar. 2015, doi: 10.1038/ncomms7649.

[12] H. Joodaki and M. B. Panzer, “Skin mechanical properties and modeling: A review,” *Proc Inst Mech Eng H*, vol. 232, no. 4, pp. 323–343, Apr. 2018, doi: 10.1177/0954411918759801.

[13] G. A. HOLZAPFEL, “Biomechanics of Soft Tissue,” in *Handbook of Materials Behavior Models*, Elsevier, 2001, pp. 1057–1071. doi: 10.1016/B978-012443341-0/50107-1.

[14] L.-R. Chang, G. Marston, and A. Martin, *Anatomy, Cartilage*. 2024.

[15] A. J. Sophia Fox, A. Bedi, and S. A. Rodeo, “The Basic Science of Articular Cartilage: Structure, Composition, and Function,” *Sports Health: A Multidisciplinary Approach*, vol. 1, no. 6, pp. 461–468, Nov. 2009, doi: 10.1177/1941738109350438.

[16] M. Oliveira Silva, J. L. Gregory, N. Ansari, and K. S. Stok, “Molecular Signaling Interactions and Transport at the Osteochondral Interface: A Review,” *Front Cell Dev Biol*, vol. 8, Aug. 2020, doi: 10.3389/fcell.2020.00750.

[17] W. R. Frontera and J. Ochala, “Skeletal Muscle: A Brief Review of Structure and Function,” *Calcif Tissue Int*, vol. 96, no. 3, pp. 183–195, Mar. 2015, doi: 10.1007/s00223-014-9915-y.

[18] N. Pien *et al.*, “Tissue engineering of skeletal muscle, tendons and nerves: A review of manufacturing strategies to meet structural and functional requirements,” *Appl Mater Today*, vol. 31, p. 101737, Apr. 2023, doi: 10.1016/j.apmt.2023.101737.

[19] P. P. Purslow, “The Structure and Role of Intramuscular Connective Tissue in Muscle Function,” *Front Physiol*, vol. 11, May 2020, doi: 10.3389/fphys.2020.00495.

[20] C. Stecco, W. Hammer, A. Vleeming, and R. De Caro, “Deep Fasciae,” in *Functional Atlas of the Human Fascial System*, Elsevier, 2015, pp. 51–102. doi: 10.1016/B978-0-7020-4430-4.00003-8.

[21] C. Gotti, A. Sensini, A. Zucchelli, R. Carloni, and M. L. Focarete, “Hierarchical fibrous structures for muscle-inspired soft-actuators: A review,” *Appl Mater Today*, vol. 20, p. 100772, Sep. 2020, doi: 10.1016/j.apmt.2020.100772.

[22] R. L. Lieber and J. Frid??n, “Clinical Significance of Skeletal Muscle Architecture,” *Clin Orthop Relat Res*, vol. 383, pp. 140–151, Feb. 2001, doi: 10.1097/00003086-200102000-00016.

[23] A. Pratesi, “Skeletal muscle: an endocrine organ,” *CLINICAL CASES IN MINERAL AND BONE METABOLISM*, 2013, doi: 10.11138/ccmbm/2013.10.1.011.

[24] W. Walsh and G. Bentley, *Repair and Regeneration of Ligaments, Tendons, and Joint Capsule*. Totowa, NJ: Humana Press, 2006. doi: 10.1385/1592599427.

[25] T. A. McMahon, *Muscles, Reflexes, and Locomotion*. Princeton: Princeton University Press, 1984.

[26] M. Shahinpoor, K. J. Kim, and M. Mojarrad, *Artificial Muscles*. CRC Press, 2007. doi: 10.1201/9781584887140.

[27] M. T. Rodrigues, R. L. Reis, and M. E. Gomes, “Engineering tendon and ligament tissues: present developments towards successful clinical products,” *J Tissue Eng Regen Med*, vol. 7, no. 9, pp. 673–686, Sep. 2013, doi: 10.1002/term.1459.

[28] M. N. Doral *et al.*, “Functional anatomy of the Achilles tendon,” *Knee Surgery, Sports Traumatology, Arthroscopy*, vol. 18, no. 5, pp. 638–643, May 2010, doi: 10.1007/s00167-010-1083-7.

[29] M. L. Osborn, J. L. Cornille, U. Blas-Machado, and E. W. Uhl, “The equine navicular apparatus as a premier enthesis organ: Functional implications,” *Veterinary Surgery*, vol. 50, no. 4, pp. 713–728, May 2021, doi: 10.1111/vsu.13620.

[30] A. Shojaee and A. Parham, “Strategies of tenogenic differentiation of equine stem cells for tendon repair: current status and challenges,” *Stem Cell Res Ther*, vol. 10, no. 1, p. 181, Dec. 2019, doi: 10.1186/s13287-019-1291-0.

[31] J. N. Fisher, A. Di Giancamillo, E. Roveda, A. Montaruli, and G. M. Peretti, “Functional Morphology of Muscles and Tendons,” in *Muscle and Tendon Injuries*, Berlin, Heidelberg: Springer Berlin Heidelberg, 2017, pp. 1–14. doi: 10.1007/978-3-662-54184-5_1.

[32] Y. Bi *et al.*, “Identification of tendon stem/progenitor cells and the role of the extracellular matrix in their niche,” *Nat Med*, vol. 13, no. 10, pp. 1219–1227, Oct. 2007, doi: 10.1038/nm1630.

[33] B. R. Freedman, J. A. Gordon, and L. J. Soslowsky, “The Achilles tendon: fundamental properties and mechanisms governing healing.,” *Muscles Ligaments Tendons J*, vol. 4, no. 2, pp. 245–55, Apr. 2014.

[34] P. W. Ackermann, P. Salo, and D. A. Hart, “Tendon Innervation.,” *Adv Exp Med Biol*, vol. 920, pp. 35–51, 2016, doi: 10.1007/978-3-319-33943-6_4.

[35] M. E. Gomes, R. L. Reis, and M. T. Rodrigues, *Tendon Regeneration: Understanding Tissue Physiology and Development to Engineer Functional Substitutes*, 1st ed. Academic Press, 2015.

[36] C. Myer and J. R. Fowler, “Flexor Tendon Repair,” *Orthopedic Clinics of North America*, vol. 47, no. 1, pp. 219–226, Jan. 2016, doi: 10.1016/j.ocl.2015.08.019.

[37] J. Buschmann and G. M. Bürgisser, *Biomechanics of Tendons and Ligaments Tissue Reconstruction and Regeneration*, 1st ed. Woodhead Publishing, 2017.

[38] J. Zabrzyński, Ł. Łapaj, Ł. Paczesny, A. Zabrzyńska, and D. Grzanka, “Tendon — function-related structure, simple healing process and mysterious ageing,” *Folia Morphol (Warsz)*, vol. 77, no. 3, pp. 416–427, Sep. 2018, doi: 10.5603/FM.a2018.0006.

[39] M. Kaya, N. Karahan, and B. Yılmaz, “Tendon Structure and Classification,” in *Tendons*, IntechOpen, 2019. doi: 10.5772/intechopen.84622.

[40] A. Sensini and L. Cristofolini, “Biofabrication of Electrospun Scaffolds for the Regeneration of Tendons and Ligaments.,” *Materials (Basel)*, vol. 11, no. 10, Oct. 2018, doi: 10.3390/ma11101963.

[41] K. L. Gohl, A. Listrat, and D. Béchet, “Hierarchical mechanics of connective tissues: integrating insights from nano to macroscopic studies.,” *J Biomed Nanotechnol*, vol. 10, no. 10, pp. 2464–507, Oct. 2014.

[42] W. Murphy, J. Black, and G. Hastings, Eds., *Handbook of Biomaterial Properties*. New York, NY: Springer New York, 2016. doi: 10.1007/978-1-4939-3305-1.

[43] T. A. L. Wren, S. A. Yerby, G. S. Beaupré, and D. R. Carter, “Mechanical properties of the human achilles tendon,” *Clinical Biomechanics*, vol. 16, no. 3, pp. 245–251, Mar. 2001, doi: 10.1016/S0268-0033(00)00089-9.

[44] K. Legerlotz, G. C. Jones, H. R. C. Screen, and G. P. Riley, “Cyclic loading of tendon fascicles using a novel fatigue loading system increases interleukin-6 expression by tenocytes,” *Scand J Med Sci Sports*, vol. 23, no. 1, pp. 31–37, Feb. 2013, doi: 10.1111/j.1600-0838.2011.01410.x.

[45] E. Maeda, S. Ye, W. Wang, D. L. Bader, M. M. Knight, and D. A. Lee, “Gap junction permeability between tenocytes within tendon fascicles is suppressed by tensile loading,” *Biomech Model Mechanobiol*, vol. 11, no. 3–4, pp. 439–447, Mar. 2012, doi: 10.1007/s10237-011-0323-1.

[46] G. M. Thornton *et al.*, “Changes in mechanical loading lead to tendonspecific alterations in MMP and TIMP expression: influence of stress deprivation and intermittent cyclic hydrostatic compression on rat supraspinatus and Achilles tendons,” *Br J Sports Med*, vol. 44, no. 10, pp. 698–703, Aug. 2010, doi: 10.1136/bjsm.2008.050575.

[47] M. Benjamin, H. Toumi, J. R. Ralphs, G. Bydder, T. M. Best, and S. Milz, “Where tendons and ligaments meet bone: attachment sites (‘entheses’) in relation to exercise and/or mechanical load,” *J Anat*, vol. 208, no. 4, pp. 471–490, Apr. 2006, doi: 10.1111/j.1469-7580.2006.00540.x.

[48] I. Calejo, R. Costa-Almeida, and M. E. Gomes, “Cellular Complexity at the Interface: Challenges in Enthesis Tissue Engineering,” 2019, pp. 71–90. doi: 10.1007/5584_2018_307.

[49] H. H. Lu and S. Thomopoulos, “Functional Attachment of Soft Tissues to Bone: Development, Healing, and Tissue Engineering,” *Annu Rev Biomed Eng*, vol. 15, no. 1, pp. 201–226, Jul. 2013, doi: 10.1146/annurev-bioeng-071910-124656.

[50] X. Zhang, D. Bogdanowicz, C. Erisken, N. M. Lee, and H. H. Lu, “Biomimetic scaffold design for functional and integrative tendon repair,” *J Shoulder Elbow Surg*, vol. 21, no. 2, pp. 266–277, Feb. 2012, doi: 10.1016/j.jse.2011.11.016.

[51] C. B. Frank, “Ligament structure, physiology and function.,” *J Musculoskelet Neuronal Interact*, vol. 4, no. 2, pp. 199–201, Jun. 2004.

[52] J. M. Oliveira and R. L. Reis, Eds., *Regenerative Strategies for the Treatment of Knee Joint Disabilities*, vol. 21. Cham: Springer International Publishing, 2017. doi: 10.1007/978-3-319-44785-8.

[53] A. Moshiri, "Tendon and Ligament Tissue Engineering, Healing and Regenerative Medicine," *J Sports Med Doping Stud*, vol. 03, no. 02, 2013, doi: 10.4172/2161-0673.1000126.

[54] P. Kannus, "Structure of the tendon connective tissue," *Scand J Med Sci Sports*, vol. 10, no. 6, pp. 312–320, Dec. 2000, doi: 10.1034/j.1600-0838.2000.010006312.x.

[55] Q. Zhang, X. Liu, L. Duan, and G. Gao, "A DNA-inspired hydrogel mechanoreceptor with skin-like mechanical behavior," *J Mater Chem A Mater*, vol. 9, no. 3, pp. 1835–1844, 2021, doi: 10.1039/D0TA11437E.

[56] X. Pan *et al.*, "A bionic tactile plastic hydrogel-based electronic skin constructed by a nerve-like nanonetwork combining stretchable, compliant, and self-healing properties," *Chemical Engineering Journal*, vol. 379, p. 122271, Jan. 2020, doi: 10.1016/j.cej.2019.122271.

[57] D. Zhang *et al.*, "Mimicking skin cellulose hydrogels for sensor applications," *Chemical Engineering Journal*, vol. 427, p. 130921, Jan. 2022, doi: 10.1016/j.cej.2021.130921.

[58] F.-L. Yi, F.-L. Guo, Y.-Q. Li, D.-Y. Wang, P. Huang, and S.-Y. Fu, "Polyacrylamide Hydrogel Composite E-skin Fully Mimicking Human Skin," *ACS Appl Mater Interfaces*, vol. 13, no. 27, pp. 32084–32093, Jul. 2021, doi: 10.1021/acsami.1c05661.

[59] B. Yang and W. Yuan, "Highly Stretchable, Adhesive, and Mechanical Zwitterionic Nanocomposite Hydrogel Biomimetic Skin," *ACS Appl Mater Interfaces*, vol. 11, no. 43, pp. 40620–40628, Oct. 2019, doi: 10.1021/acsami.9b14040.

[60] Y. A. Ismail, J. G. Martínez, A. S. Al Harrasi, S. J. Kim, and T. F. Otero, "Sensing characteristics of a conducting polymer/hydrogel hybrid microfiber artificial muscle," *Sens Actuators B Chem*, vol. 160, no. 1, pp. 1180–1190, Dec. 2011, doi: 10.1016/j.snb.2011.09.044.

[61] S. Y. Zheng *et al.*, "Programmed Deformations of 3D-Printed Tough Physical Hydrogels with High Response Speed and Large Output Force," *Adv Funct Mater*, vol. 28, no. 37, Sep. 2018, doi: 10.1002/adfm.201803366.

[62] F. Zhu *et al.*, "3D Printing of Ultratough Polyion Complex Hydrogels," *ACS Appl Mater Interfaces*, vol. 8, no. 45, pp. 31304–31310, Nov. 2016, doi: 10.1021/acsami.6b09881.

[63] F. Zhu *et al.*, "Tough polyion complex hydrogel films of natural polysaccharides," *Chinese Journal of Polymer Science*, vol. 35, no. 10, pp. 1276–1285, Oct. 2017, doi: 10.1007/s10118-017-1977-7.

[64] H. Qin, T. Zhang, N. Li, H.-P. Cong, and S.-H. Yu, "Anisotropic and self-healing hydrogels with multi-responsive actuating capability," *Nat Commun*, vol. 10, no. 1, p. 2202, May 2019, doi: 10.1038/s41467-019-10243-8.

[65] N. Ding *et al.*, "Mimicking the Mechanical Properties of Cartilage Using Ionic- and Hydrogen-Bond Cross-Linked Hydrogels with a High Equilibrium Water Content above 70%," *ACS Appl Polym Mater*, vol. 3, no. 5, pp. 2709–2721, May 2021, doi: 10.1021/acsapm.1c00264.

[66] Q. Chen *et al.*, "Bilayer Hydrogels with Low Friction and High Load-Bearing Capacity by Mimicking the Oriented Hierarchical Structure of Cartilage," *ACS Appl Mater Interfaces*, vol. 14, no. 46, pp. 52347–52358, Nov. 2022, doi: 10.1021/acsami.2c13641.

[67] C. Luo, A. Guo, J. Li, Z. Tang, and F. Luo, "Janus Hydrogel to Mimic the Structure and Property of Articular Cartilage," *ACS Appl Mater Interfaces*, vol. 14, no. 31, pp. 35434–35443, Aug. 2022, doi: 10.1021/acsami.2c09706.

[68] S. Choi, Y. Choi, and J. Kim, "Anisotropic Hybrid Hydrogels with Superior Mechanical Properties Reminiscent of Tendons or Ligaments," *Adv Funct Mater*, vol. 29, no. 38, Sep. 2019, doi: 10.1002/adfm.201904342.

[69] S. Choi *et al.*, "Bone-Adhesive Anisotropic Tough Hydrogel Mimicking Tendon Enthesis," *Advanced Materials*, vol. 35, no. 3, Jan. 2023, doi: 10.1002/adma.202206207.

[70] P. Wei *et al.*, "Strong and Tough Cellulose Hydrogels via Solution Annealing and Dual Cross-Linking," *Small*, vol. 19, no. 28, Jul. 2023, doi: 10.1002/smll.202301204.

[71] Y. Wu *et al.*, "Solvent-Exchange-Assisted Wet Annealing: A New Strategy for Superstrong, Tough, Stretchable, and Anti-Fatigue Hydrogels," *Advanced Materials*, p. 2210624, Mar. 2023, doi: 10.1002/adma.202210624.

[72] N. Park and J. Kim, "Anisotropic Hydrogels with a Multiscale Hierarchical Structure Exhibiting High Strength and Toughness for Mimicking Tendons," *ACS Appl Mater Interfaces*, vol. 14, no. 3, pp. 4479–4489, Jan. 2022, doi: 10.1021/acsami.1c18989.

[73] S. Lin *et al.*, "Anti-fatigue-fracture hydrogels," *Sci Adv*, vol. 5, no. 1, Jan. 2019, doi: 10.1126/sciadv.aau8528.

[74] A. K. Means, C. S. Shrode, L. V. Whitney, D. A. Ehrhardt, and M. A. Grunlan, "Double Network Hydrogels that Mimic the Modulus, Strength, and Lubricity of Cartilage," *Biomacromolecules*, vol. 20, no. 5, pp. 2034–2042, May 2019, doi: 10.1021/acs.biomac.9b00237.

[75] Q. Chen *et al.*, "Anisotropic hydrogels with enhanced mechanical and tribological performance by magnetically oriented nanohybrids," *Chemical Engineering Journal*, vol. 430, p. 133036, Feb. 2022, doi: 10.1016/j.cej.2021.133036.

[76] P. D. Topham, J. R. Howse, C. J. Crook, S. P. Armes, R. A. L. Jones, and A. J. Ryan, "Antagonistic Triblock Polymer Gels Powered by pH Oscillations," *Macromolecules*, vol. 40, no. 13, pp. 4393–4395, Jun. 2007, doi: 10.1021/ma071041j.

[77] M. Bassil, M. Ibrahim, and M. El Tahchi, "Artificial muscular microfibers: hydrogel with high speed tunable electroactivity," *Soft Matter*, vol. 7, no. 10, p. 4833, 2011, doi: 10.1039/c1sm05131h.

[78] Z. Sun, L. Yang, J. Zhao, and W. Song, "Natural Cellulose-Full-Hydrogels Bioinspired Electroactive Artificial Muscles: Highly Conductive Ionic Transportation Channels and Ultrafast Electromechanical Response," *J Electrochem Soc*, vol. 167, no. 4, p. 047515, Feb. 2020, doi: 10.1149/1945-7111/ab732e.

[79] J. Wu, Y. Lin, and J. Sun, "Anisotropic volume change of poly(N-isopropylacrylamide)-based hydrogels with an aligned dual-network microstructure," *J Mater Chem*, vol. 22, no. 34, p. 17449, 2012, doi: 10.1039/c2jm34010k.

[80] A. Sydney Gladman, E. A. Matsumoto, R. G. Nuzzo, L. Mahadevan, and J. A. Lewis, "Biomimetic 4D printing," *Nat Mater*, vol. 15, no. 4, pp. 413–418, Apr. 2016, doi: 10.1038/nmat4544.

[81] S. Hong *et al.*, "3D Printing: 3D Printing of Highly Stretchable and Tough Hydrogels into Complex, Cellularized Structures (Adv. Mater. 27/2015)," *Advanced Materials*, vol. 27, no. 27, pp. 4034–4034, Jul. 2015, doi: 10.1002/adma.201570182.

[82] Y. Xia *et al.*, "Multifunctional Glycerol–Water Hydrogel for Biomimetic Human Skin with Resistance Memory Function," *ACS Appl Mater Interfaces*, vol. 11, no. 23, pp. 21117–21125, Jun. 2019, doi: 10.1021/acsami.9b05554.

[83] J. Zhang *et al.*, "Hydrogel from Chrome Shavings as a Sustainable, Highly Sensitive Ionic Skin for Pressure Sensing," *ACS Sustain Chem Eng*, vol. 10, no. 25, pp. 8172–8183, Jun. 2022, doi: 10.1021/acssuschemeng.2c01421.

[84] M. Jo *et al.*, "Protein-Based Electronic Skin Akin to Biological Tissues," *ACS Nano*, vol. 12, no. 6, pp. 5637–5645, Jun. 2018, doi: 10.1021/acsnano.8b01435.

[85] S. H. Tan, D. A. C. Chua, J. R. J. Tang, C. Bonnard, D. Leavesley, and K. Liang, "Design of hydrogel-based scaffolds for in vitro three-dimensional human skin model reconstruction," *Acta Biomater*, vol. 153, pp. 13–37, Nov. 2022, doi: 10.1016/j.actbio.2022.09.068.

[86] B. S. Kwak *et al.*, "In vitro 3D skin model using gelatin methacrylate hydrogel," *Journal of Industrial and Engineering Chemistry*, vol. 66, pp. 254–261, Oct. 2018, doi: 10.1016/j.jiec.2018.05.037.

[87] W. Wang *et al.*, “Extracellular matrix mimicking dynamic interpenetrating network hydrogel for skin tissue engineering,” *Chemical Engineering Journal*, vol. 457, p. 141362, Feb. 2023, doi: 10.1016/j.cej.2023.141362.

[88] “Research Highlights,” *Nat Biotechnol*, vol. 34, no. 9, pp. 932–932, Sep. 2016, doi: 10.1038/nbt.3668.

[89] M. Liu *et al.*, “Injectable hydrogels for cartilage and bone tissue engineering,” *Bone Res*, vol. 5, no. 1, p. 17014, May 2017, doi: 10.1038/boneres.2017.14.

[90] N. Annabi, K. Yue, A. Tamayol, and A. Khademhosseini, “Elastic sealants for surgical applications,” *European Journal of Pharmaceutics and Biopharmaceutics*, vol. 95, pp. 27–39, Sep. 2015, doi: 10.1016/j.ejpb.2015.05.022.

[91] F. Qiu, X. Fan, W. Chen, C. Xu, Y. Li, and R. Xie, “Recent Progress in Hydrogel-Based Synthetic Cartilage: Focus on Lubrication and Load-Bearing Capacities,” *Gels*, vol. 9, no. 2, p. 144, Feb. 2023, doi: 10.3390/gels9020144.

[92] Y. S. Zhang and A. Khademhosseini, “Advances in engineering hydrogels,” *Science (1979)*, vol. 356, no. 6337, May 2017, doi: 10.1126/science.aaf3627.

[93] C. B. Highley, C. B. Rodell, and J. A. Burdick, “Direct 3D Printing of Shear-Thinning Hydrogels into Self-Healing Hydrogels,” *Advanced Materials*, vol. 27, no. 34, pp. 5075–5079, Sep. 2015, doi: 10.1002/adma.201501234.

[94] N. Annabi *et al.*, “25th Anniversary Article: Rational Design and Applications of Hydrogels in Regenerative Medicine,” *Advanced Materials*, vol. 26, no. 1, pp. 85–124, Jan. 2014, doi: 10.1002/adma.201303233.

[95] E. R. Ruskowitz and C. A. DeForest, “Photoresponsive biomaterials for targeted drug delivery and 4D cell culture,” *Nat Rev Mater*, vol. 3, no. 2, p. 17087, Jan. 2018, doi: 10.1038/natrevmats.2017.87.

[96] M. Chen, Y. Cui, Y. Wang, and C. Chang, “Triple physically cross-linked hydrogel artificial muscles with high-stroke and high-work capacity,” *Chemical Engineering Journal*, vol. 453, p. 139893, Feb. 2023, doi: 10.1016/j.cej.2022.139893.

[97] J. Hu, S. Liu, and C. Fan, “Applications of functionally-adapted hydrogels in tendon repair,” *Front Bioeng Biotechnol*, vol. 11, Feb. 2023, doi: 10.3389/fbioe.2023.1135090.

[98] Y. Tang, Z. Wang, L. Xiang, Z. Zhao, and W. Cui, “Functional biomaterials for tendon/ligament repair and regeneration,” *Regen Biomater*, vol. 9, Apr. 2022, doi: 10.1093/rb/rbac062.

[99] X. Tang, L. Daneshmandi, G. Awale, L. S. Nair, and C. T. Laurencin, “Skeletal Muscle Regenerative Engineering,” *Regen Eng Transl Med*, vol. 5, no. 3, pp. 233–251, Sep. 2019, doi: 10.1007/s40883-019-00102-9.

[100] Y. Yuryev and P. Wood-Adams, “Rheological properties of crystallizing polylactide: Detection of induction time and modeling the evolving structure and properties,” *J Polym Sci B Polym Phys*, vol. 48, no. 7, pp. 812–822, Apr. 2010, doi: 10.1002/polb.21953.

[101] S. Suganthi, S. Vignesh, J. Kalyana Sundar, and V. Raj, “Fabrication of PVA polymer films with improved antibacterial activity by fine-tuning via organic acids for food packaging applications,” *Appl Water Sci*, vol. 10, no. 4, p. 100, Apr. 2020, doi: 10.1007/s13201-020-1162-y.

[102] Q. Liu, N. Chen, S. Bai, and W. Li, “Effect of silver nitrate on the thermal processability of poly(vinyl alcohol) modified by water,” *RSC Adv*, vol. 8, no. 5, pp. 2804–2810, 2018, doi: 10.1039/C7RA12941F.

[103] R. P. F. de Sousa *et al.*, “Formulation and Study of an Environmentally Friendly Microemulsion-Based Drilling Fluid (O/W) with Pine Oil,” *Energies (Basel)*, vol. 14, no. 23, p. 7981, Nov. 2021, doi: 10.3390/en14237981.

[104] TA Instruments, “Interpreting Unexpected Events and Transitions in DSC Results,” *TA Instruments*.

[105] M. Mohsin, A. Hossin, and Y. Haik, “Thermal and mechanical properties of poly(vinyl alcohol) plasticized with glycerol,” *J Appl Polym Sci*, vol. 122, no. 5, pp. 3102–3109, Dec. 2011, doi: 10.1002/app.34229.

[106] K. Ou, X. Dong, C. Qin, X. Ji, and J. He, “Properties and toughening mechanisms of PVA/PAM double-network hydrogels prepared by freeze-thawing and anneal-swelling,” *Materials Science and Engineering: C*, vol. 77, pp. 1017–1026, Aug. 2017, doi: 10.1016/j.msec.2017.03.287.

[107] D. Hu *et al.*, “Dual-physical network PVA hydrogel commensurate with articular cartilage bearing lubrication enabled by harnessing nanoscale crystalline domains,” *Nano Res*, Sep. 2024, doi: 10.1007/s12274-024-6968-8.

Appendix A – Yield Point Determination

This appendix presents the graphs of the standardized residuals in the linear segment of one compression curve and how it relates to the selection of the yield point.

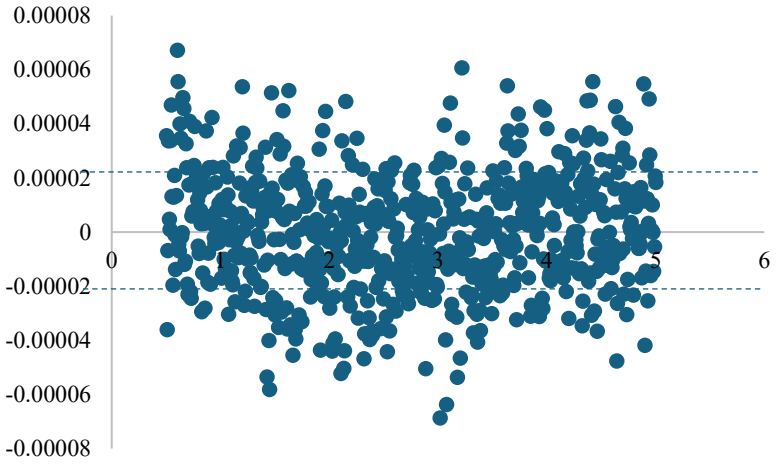

Standardized residuals of the linear segment of one compression curve.

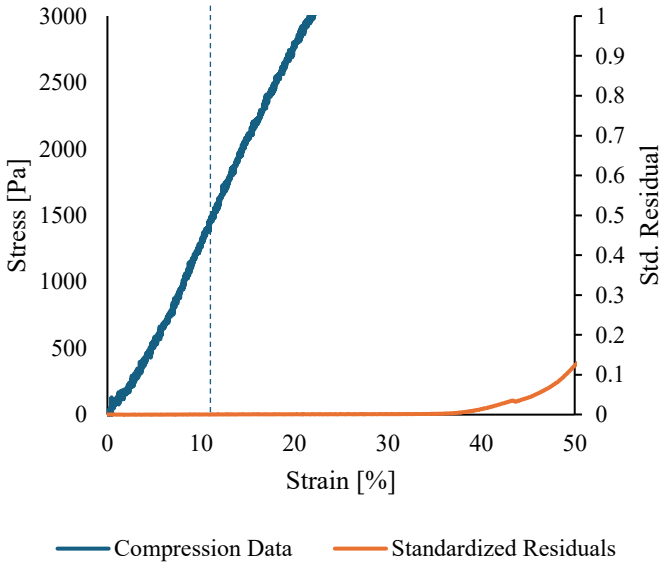

Compression results of one curve compared to its standardized residuals, with the yield point identified by a dashed line.

Appendix B – Statistical Analysis

This appendix contains the results of the one-way ANOVA analyses conducted for the data contained in Chapter 3, as well as the Tukey post-hoc analysis. All analyses were done in SPSS.

ANOVA

		Sum of Squares	df	Mean Square	F	Sig.
CompModulus	Between Groups	1639510.370	4	409877.592	3.604	.015
	Within Groups	3981013.157	35	113743.233		
	Total	5620523.527	39			
YieldStrength	Between Groups	43832095.042	4	10958023.760	5.712	.001
	Within Groups	67147859.227	35	1918510.264		
	Total	110979954.27	39			

CompModulus

Tukey HSD[a]

AnnTimes	N	Subset for alpha = 0.05	
		1	2
.00	8	27.7775	
30.00	8	78.2467	
60.00	8	145.1418	145.1418
120.00	8	361.1724	361.1724
90.00	8		571.8217
Sig.		.298	.107

Means for groups in homogeneous subsets are displayed.

a. Uses Harmonic Mean Sample Size = 8.000.

YieldStrength

Tukey HSD[a]

AnnTimes	N	Subset for alpha = 0.05	
		1	2
.00	8	650.2365	
30.00	8	1210.5396	
60.00	8	1610.8507	
120.00	8	2445.3003	2445.3003
90.00	8		3649.7649
Sig.		.094	.424

Means for groups in homogeneous subsets are displayed.

a. Uses Harmonic Mean Sample Size = 8.000.

One way ANOVA and Tukey post-hoc results for the compressive modulus and yield strength across different annealing times.

ANOVA

		Sum of Squares	df	Mean Square	F	Sig.
Tm	Between Groups	9.768	4	2.442	.126	.970
	Within Groups	194.086	10	19.409		
	Total	203.854	14			
Tc	Between Groups	3.283	4	.821	.046	.995
	Within Groups	180.379	10	18.038		
	Total	183.662	14			

Tm

Tukey HSD[a]

AnnTimes	N	Subset for alpha = 0.05 1
120	3	221.5467
90	3	222.2100
60	3	222.9333
30	3	223.0267
0	3	223.9367
Sig.		.960

Means for groups in homogeneous subsets are displayed.

a. Uses Harmonic Mean Sample Size = 3.000.

Tc

Tukey HSD[a]

AnnTimes	N	Subset for alpha = 0.05 1
90	3	195.2600
120	3	195.6900
60	3	195.8733
30	3	196.3000
0	3	196.6000
Sig.		.994

Means for groups in homogeneous subsets are displayed.

a. Uses Harmonic Mean Sample Size = 3.000.

One way ANOVA and Tukey post-hoc results for melting and crystallization peak temperatures across different annealing times.

ANOVA

		Sum of Squares	df	Mean Square	F	Sig.
Diameter	Between Groups	181.865	1	181.865	415.688	<.001
	Within Groups	7.875	18	.438		
	Total	189.740	19			
Thickness	Between Groups	6.682	1	6.682	70.340	<.001
	Within Groups	1.710	18	.095		
	Total	8.392	19			

One way ANOVA results for the dimensions of the initial hydrogel and organogel.